Advanced Drug Delivery Reviews 72 (2014) 127–143

Contents lists available at ScienceDirect

Advanced Drug Delivery Reviews

journal homepage: www.elsevier.com/locate/addr

Ultrasound mediated transdermal drug delivery ☆

Aharon Azagury [a], Luai Khoury [b], Giora Enden [b], Joseph Kost [a,*]

[a] Department of Chemical Engineering, Ben-Gurion University, Beer-Sheva 84105, Israel
[b] Department of Biomedical Engineering, Ben-Gurion University, Beer-Sheva 84105, Israel

ARTICLE INFO

Available online 22 January 2014

Keywords:
Sonophoresis
Transdermal drug delivery
Ultrasound
Transport phenomena
Models and simulations
Synergistic effects of ultrasound
Safety

ABSTRACT

Transdermal drug delivery offers an attractive alternative to the conventional drug delivery methods of oral administration and injections. However, the stratum corneum serves as a barrier that limits the penetration of substances to the skin. Application of ultrasound (US) irradiation to the skin increases its permeability (sonophoresis) and enables the delivery of various substances into and through the skin.
This review presents the main findings in the field of sonophoresis in transdermal drug delivery as well as transdermal monitoring and the mathematical models associated with this field. Particular attention is paid to the proposed enhancement mechanisms and future trends in the fields of cutaneous vaccination and gene therapy.

Contents

☆ This review is part of the *Advanced Drug Delivery Reviews* theme issue on "Ultrasound triggered drug delivery".

* Corresponding author at: Department of Chemical Engineering, Ben-Gurion University of the Negev, POB 653, Beer-Sheva 84105, Israel. Tel.: +972 8 646 1212/3; fax: +972 8 646 1023.
E-mail address: kost@bgu.ac.il (J. Kost).

0169-409X/$ – see front matter
http://dx.doi.org/10.1016/j.addr.2014.01.007

1. Introduction

Effective therapeutic outcome requires not only proper drug selection but also an effective drug delivery system. The human skin is a readily accessible surface for drug delivery. Transdermal drug delivery—the delivery of drugs across the skin and into systemic circulation—is distinct from topical drug administration, which targets local areas. Transdermal drug delivery offers several important advantages over more traditional dosage forms such as oral delivery and injections, including elimination of first pass metabolism and minimization of pain. The steady permeation of a drug across the skin allows for long-lasting and more consistent serum drug levels, often a goal of therapy [1]. (See Table 1.)

In spite of major research and development efforts in transdermal systems and the many advantages of the transdermal route, low permeability of the human skin remains a major hurdle that limits the usefulness of the transdermal delivery approach. It is well accepted that the stratum corneum (SC), the uppermost layer of the skin, is the major rate-limiting barrier to molecular diffusion through the mammalian epidermis. Due to the fact that most drugs do not permeate the skin in therapeutic quantities, chemical and physical approaches have been examined to transiently lower the SC barrier properties and enhance transdermal transport. Illustrating the problem is the fact that as of today, drugs that are administered across the skin are of low molecular mass (<500 Da) and very lipophilic in nature at low dosages [1]. Hydrophilic solutes generally exhibit poor skin permeability (10^{-7}–10^{-8} cm/s), about one or more orders of magnitude lower than hydrophobic solutes [2].

For protein and peptide drugs, the transdermal route has the potential of being an extremely efficient delivery domain. Topical application avoids the effects of both gastric degradation and hepatic first-pass metabolism; it presents a large surface area for absorption (approximately 2 m^2) and has relatively low proteolytic activity. The skin is undoubtedly one of the most easily accessible organs of the body. Of course, as mentioned above, the molecular size of the transported agents precludes their passive delivery through skin at effective therapeutic concentrations.

The chemical approach using chemical penetration enhancers (CPEs) for enhancement of transdermal mass transport has long been used, especially in cosmetics. CPEs are divided into chemical groups such as: sulfoxides, pyrrolidones, fatty acids, alcohols, surfactants, metabolic interventions, and the only specifically designed material designated to enhance transdermal mass transport, Azone. Most CPEs enhance transdermal mass transport by interacting with the intercellular lipid domain of the SC. Although many chemicals have been evaluated as CPEs in human or animal skins, to-date none has proven to be ideal because of suspected pharmacological activity or unresolved safety issues [3].

Table 1
Absorption coefficients (α) at 1 MHz Ultrasound for various organs [28].

Material	α (dB/cm)
Blood	0.18
Lung	40
Liver	0.9
Brain	0.85
Kidney	1.0
Spinal cord	1.0
Lens of eye	2.0
Skull bone	20
Fat	0.6
Muscle (across fibers)	3.3
Muscle (along fibers)	1.2
Water	0.0022

Several physical approaches for skin penetration enhancement, such as stripping of the SC, micro-needles, heating, iontophoresis, electroporation, and ultrasound have also been evaluated [4].

1.1. Micro-needles

Micro-needles are designed to create a physical pathway through the upper epidermis to increase skin permeability. They are applied to the skin surface and pierce the outer epidermis layer (which contains no nerves) deep enough to increase skin permeability and allow drug delivery, but superficially enough not to cause any pain through the sensory receptors of the dermis. For example, individual silicon needles 150 μm in length and 80 μm in base diameter are fabricated onto arrays of 3 × 3 mm (approximately 400 needles), or needles with hollow centers, each containing a bore of 5–70 μm through which drugs can be administered [5].

1.2. Laser cell-ablation

Laser cell-ablation to remove the SC barrier by controlled ablation has also been investigated as a means of enhancing topical drug delivery. Laser such as erbium – yttrium-aluminum-garnet (YAG) – was found to increase skin permeability. The molecular size, lipophilicity, and sequence of the peptides were found to play important roles in modulating the delivery enhancement. In an in vivo study, mouse skin was treated with laser followed by skin vaccination with a lysozyme antigen. It was demonstrated that laser treatment with no adjuvant or penetration enhancer enhanced the production of antibodies in the serum 3-fold [6].

1.3. Radio-frequency (RF) cell-ablation

Radio-frequency (RF) cell-ablation is performed by placing an array of microelectrodes on a body area (i.e., skin) and passing an alternating electrical current at a frequency of 100–500 kHz (radio frequency) through the area. The ions in the cells adjacent to the microelectrodes vibrate as they try to follow the change in electrical current direction. These vibrations generate heat, which causes water evaporation, cell ablation, and possibly damage of deeper skin layers. RF micro-channels are created by placing a closely spaced array of tiny electrodes with very precise dimensions against the skin. The alternating electrical current is transferred through each of the microelectrodes, ablates the cells underneath each electrode, and forms microscopic passages in the SC and in the outer dermis [7,8].

1.4. Iontophoresis (IP)

The iontophoretic method is based on the repulsion forces of same charges. It involves the application of small electric current (up to 0.5 mA/cm^2) to a drug reservoir wetting the surface of the skin, with the same charged electrode as the solute of interest. This produces repulsion that effectively drives the solute molecules across the SC towards the opposite electrode, which is placed elsewhere on the body [9]. Iontophoresis can enhance the penetration of uncharged molecules into the skin as well. When an electric field is applied to a solution consisting of charged ions, the charged ions are forced to move in the direction of the field. Due to viscous forces the entire solution undergoes a convective flow that carries non-charged particles as well. This process is referred to as electro-osmosis [10].

1.5. Electroporation

Electroporation, originally used to transfect cells with macromolecules such as DNA, involves the application of a pulsating electrical field at high voltage (>50 V, typically 1–100 ms) to the skin. This causes the formation of transient aqueous pores in the SC, through which

molecular transport is attainable. Electroporation leads to enhanced skin permeability, mainly attributed to electrophoretic movement and diffusion through the newly created aqueous pathways [11]. Although electroporation involves the application of an electric field similar to that of iontophoresis, the enhanced transports in these procedures are based on a different principle. While iontophoresis directly acts on the drug molecule to propel it into the skin, electroporation acts mainly on the skin to increase its permeability [12].

1.6. Electroporation

Ultrasound, phonophoresis, or sonophoresis is defined as the transport of drugs through the skin and into the soft tissue during or following the influence of an ultrasonic perturbation. In this review we present sonophoresis experimental results, clinical studies, and theoretical models associated with novel conceptual insights [13–15]. Ultrasound frequencies used in medicine can vary from 20 kHz to 16 MHz [16]. Lower and medium range ultrasound frequencies (20–200 kHz and 0.2–1 MHz, respectively) are predominantly used for sonophoresis purposes due to their relatively higher cavitational effects (more detail in Section 2). Traditionally, higher ultrasound frequencies are also used for imaging, physiotherapy, and for gallstone and kidney stone pulverization.

2. Biological effects of ultrasound

Ultrasound has long been used for medical purposes in a wide range of frequencies. Examples include: ultrasonic tomography and imaging, and the detection of abnormalities by utilizing a pulsed echo (wavelength of approximately 10^{-4} m) [17]. The use of ultrasound (specifically HIFU) is gaining rapid clinical acceptance as a treatment modality enabling non-invasive tissue heating and ablation in numerous applications in radiation therapy such as tumor therapy lithotripsy, ultrasound-assisted lipoplasty, and ultrasonic surgical instruments [18]. Ultrasound has also been used to enhance uptake of drugs, proteins, DNA/RNA, and other compounds into cells and tissues [19–22].

Assessing the biological effects of ultrasound on tissues and cells has been investigated thoroughly. It has been commonly believed for decades that ultrasound effects on tissues and cells are mainly through three mechanisms: cavitational (mainly inertial cavitation), thermal and acoustic streaming [23]. Recently Krasovitski et al. [24] proposed a new, non-thermal and non-cavitational mechanism for ultrasound effects on biological tissues. Ultrasound can also induce other effects in liquids that researchers should take into account, specifically sonochemistry [25].

2.1. Thermal effects

Ultrasound can increase insonated medium's temperature by the absorption of the sound waves. Obviously, the higher is the medium's absorption coefficient, the higher the increase in temperature and thus in thermal effect. For example, the bone is an organ that possesses high ultrasound absorption coefficients while the muscle tissue has a low absorption coefficient [26]. This is why using ultrasound on the brain still presents a great challenge. The increase in the medium's temperature upon ultrasound exposure at a given frequency varies directly with ultrasound intensity and exposure time. The absorption coefficient of a material/organ increases directly with ultrasound frequency, resulting in a greater temperature increase for the same intensity. For example, liver absorption coefficient, which at 0.5 MHz equals 0.01 neper/cm, becomes 0.24 neper/cm at 7 MHz [27].

2.2. Cavitational effects

Cavitation may be defined as the formation of bubbles in an insonated medium. These bubbles are formed mainly due to ultrasound-induced pressure changes in the medium. Cavitation is divided into two categories: inertial and stable. In inertial cavitation the bubble grows rapidly and then collapses when it reaches a certain diameter (depending mainly on the ultrasound frequency). On the other hand, stable cavitation concerns stably oscillating bubbles in the ultrasound field. The bubble collapse results in extreme conditions in its vicinity, due to sonochemical reactions. These conditions reach temperatures of above 5000 K [29] and pressures of about 300 bar [30]. The bubble collapse induces shock waves that may cause structural shifts to the surrounding tissues by micro-jets, resulting from non-symmetrical bubble collapse that induces convection. Cavitation does not occur at all intensities; threshold intensity is needed. Once the intensity threshold is surpassed, the higher the intensity the greater the cavitational effect. The intensity threshold for cavitation increases with increasing ultrasound frequency, ambient pressure, medium viscosity, surface tension, and ion concentration. On the other hand, cavitation threshold intensity decreases with increasing medium temperature and gas content [26]. Thus, increased cavitational effect may be achieved by using low-frequency ultrasound and gassy fluids, and when surfactants are added to the medium.

Cavitation effects may also be increased by using ultrasound contrast agents (UCA, also used for ultrasound imaging). Park et al. found that when adding 0.1% UCA Definity® to the insonated medium (ultrasound frequency of 1 MHz) for the delivery of glycerol across porcine skin, the enhancement effect increased from 3-fold to 5-fold compared to passive diffusion [31] for ultrasound and UCA + ultrasound, respectively. Park et al. also demonstrated that this combination can be used in vivo in a rat model using higher ultrasound frequencies but for 30 min rather than to 60 min for the in vitro system [32], for enhancing the mass transport of molecular masses of 4, 20, and 150 kDa.

Polat et al. [33], in their review, suggest different cavitational mechanism effects on skin depending on ultrasound frequency. The authors also emphasize that this difference has not been accounted for in many cases, resulting in wrong analysis of the results. They argue that at low frequency ultrasound (20–100 kHz) cavitational bubbles are created near the skin, while at high frequency ultrasound (>0.7 MHz) the cavitational bubbles are created within the skin (due to smaller resonant bubble diameter) inside inherent cavities such as hair follicle shafts, and sweat glands. The relation between bubble radius size and ultrasound frequency may be calculated by the Plesset and Prosperetti equation [34] both of which can be reduced to Eq. (1) (when inserting the properties of the medium and gas content):

$$R_b = \frac{\alpha}{f}, \tag{1}$$

where R_b is the bubble radius, α is a constant depending on medium properties and gas content (for an air-water system α is 3–4 m/s), and f is the ultrasound frequency (in Hz) [35]. For example, bubble radius reduces from 150 μm to 2.7 μm for frequencies of 20 kHz and 1.1 MHz, respectively. However, experimental results show that bubble size is not univalent and may vary; moreover, the measured mean bubble size is lower than the calculated value from theory (i.e., experimental radius of 3.2 μm compared to 8.5 μm theoretical result at 355 kHz [36]). This information should be taken into account in sonophoresis mechanism studies when cavities are known-to-exist.

2.3. Acoustic streaming effects

Acoustic streaming is the development of unidirectional flow currents in a fluid generated by sound waves. Ultrasound reflections and other distortions that occur during wave propagations are the main cause of acoustic streaming. Acoustic streaming may also be enhanced by the oscillations of the cavitational bubbles. Adjacent tissue structures might be affected by the shear stresses developed by streaming velocities. Acoustic streaming might play a significant role when the medium

has an acoustic impedance that differs from that of its surroundings. To date, the potential clinical value of acoustic streaming has only been minimally explored. Some researchers distinguish between "bulk-streaming" and "micro-streaming" in terms of their intensity, implying that micro-streaming is more powerful than bulk-streaming. Bulk-streaming is the movement of the insonated fluid in a single direction (as the ultrasound wave), whereas micro-streaming forms from an oscillating source inducing swirls of flow. Since micro-streaming is more powerful it is argued that it is the only type of acoustic streaming powerful enough to indeed alter membrane permeability and stimulate cell activity [37].

2.4. Bilayer sonophore effect

The BLS model suggested by Krasovitski et al. [24] accounts for observed non-thermal ultrasound effects at intensities below the cavitational threshold [38–40], but the authors indicate that the model may also explain cavitational effects. More importantly, this model suggests a different mechanism for the increased permeability induced by ultrasound that until recently was explained solely by extracellular cavitation. Traditionally, these effects were attributed mainly to mechanical effects associated with cavitation and micro-streaming. Their model is based on the direct effect of ultrasonic pressure waves on bilayer membranes. The acoustic pressure oscillates between compression (positive) and rarefaction (negative) values. At the negative pressure phase, the space between the two membrane leaflets increases (pushing away the surrounding medium) and decreases at the positive pressure phase. As a result, the continuity of the membrane is transiently interrupted and pores are created through which substances are transported across the membrane. For a full description of the model and its assumptions see [24].

2.5. Effect on skin

Various researches have reported histological studies of insonated skin [41–44] under various ultrasound conditions to assess the ultrasound effect on living skin cells. Sekkat et al. [41] evaluated the SC barrier function of the porcine ear during its progressive removal by adhesive tape stripping, in terms of biophysical parameters such as diffusivity, permeability, and the product of ionic partition coefficient and mobility determined by a trans-epidermal water loss technique (TEWL) and skin impedance measurements. They found that TEWL increased slowly at first and then rapidly with progressive SC removal. In contrast, low-frequency skin impedance decreased with SC stripping. They compared their results with previously published results for human in vivo skin studies and showed that porcine ear skin in vitro can be used as a valid model for humans [41].

Histological studies of hairless rat skin exposed to therapeutic ultrasound were performed by Levy et al. [45] in which they reported that application of ultrasound (1 MHz, 2 W/cm^2) induced no damage to rat's skin. Similar results were observed by Tachibana [46] on insonated rabbit skin. Tachibana [46] also reported no damage to the skin upon low-frequency ultrasound application (105 kHz, 5000 Pa pressure amplitude). Mitragotri et al. [47,48] performed histological studies of hairless rat skin exposed to low-frequency ultrasound (20 kHz, 12.5–225 mW/cm^2) and found no damage to the epidermis and underlying living tissues. Yamashita et al. [49] investigated the effects of ultrasound at a frequency of 48 kHz (0.5 W/cm^2) on the surface of hairless mouse and human skin by utilizing scanning electron microscopy. They reported that the effect of ultrasound was much less significant on human skin than on mouse skin. Following the exposure to ultrasound, human skin exhibited some removal of keratinocytes around hair follicles whereas the outer layer of mouse SC was totally removed and pores were observed. Cavitation was determined as the main effect in these experiments. The effect of low-frequency ultrasound (20 kHz) on hairless mouse skin and human skin was also investigated by Boucaud et al. [50]. Human skin samples exposed to low-intensity ultrasound (<2.5 W/cm^2) showed no histological change. Further microscopic examination using transmission electron microscopy confirmed a lack of structural modification.

All these experiments suggest that the ultrasound parameters that affect skin permeability are the exposure duration, frequency, and intensity.

2.6. Other ultrasound applications

Ultrasound has been used extensively to enhance transdermal drug delivery, and has also been used on skin for other applications. For example, Voigt et al. [51] used ultrasound (20–30 kHz) as adjunctive treatment to improve the healing of chronic wounds. It is believed that the debridement of adherent necrotic fibrin, loose slough, and fragmentation of bacteria and biofilms on wound surfaces is affected by ultrasound exposure [52]. Debridement can help in the healing process since it removes necrotic tissue that serves as medium for bacterial growth and since this tissue also forms a physical barrier to granulation, contraction, and epithelization in the wound bed [51,53]. Another example is the use of therapeutic ultrasound for reducing localized fat deposits to improve body contours. Moreno-Moraga et al. [54] showed that using an ultrasound system (UltraShape Ltd., Tel Aviv, Israel, frequency 200 ± 30 kHz, and intensity 17.5 W/cm^2) on patients' skin regions, such as abdomen and inner and outer thighs, induced a decrease in fat thickness after three treatments (one month intervals) by 2.28 ± 0.80 cm. However, the duration of insonation was not mentioned and the authors simply reported that the duration was determined by the embedded feedback system in the apparatus. The reported results claimed a reduction in body circumference by a mean of 3.95 ± 1.99 cm. Ascher showed similar results using the same system on Caucasian women (circumference reduced by 3.58 cm) [55]. On the other hand, Shek et al. used the same system on 53 patients (51 females and 2 males) and found no effect on abdominal circumference and also reported poor satisfaction among patients [56].

Ultrasound has also been used in other cosmetic applications. For example, in facial plastic surgery, White et al. [57] (in vitro) and Gliklich et al. [44] (clinical) showed that high frequency ultrasound (7.5 and 4.4 MHz, respectively) may be targeted to induce thermal injury zones (TIZ). Noninvasive rejuvenation treatments are based on the ability to produce TIZs that trigger tissue remodeling and/or tightening (i.e., mini face lift surgery) [44,58].

3. Use of ultrasound in transdermal drug delivery

Fellinger and Schmidt were the first to report back in 1950 [59] on the successful treatment of polyarthritis of the hand's digital joints using hydrocortisone ointment with sonophoresis. However, the first ultrasound device approved by the FDA was only in 2004 for the application of local dermal anesthesia of lidocaine [60]. With the development of transdermal delivery, as an important means of systemic drug administration, researchers have been investigating possible application of ultrasound in transdermal drug delivery systems [45]. Ultrasound (with and without other enhancement methods) has been assessed and its effect well established at various frequencies using various molecules [33,42,50,61–80]. Ultrasound has also been used to effectively enable the transdermal mass transport of cationic, neutral, and anionic quantum dots (10 nm and 20 nm) and gold nanoparticles (~5 nm) using 20 kHz ultrasound at 7.5 W/cm^2 with 1% w/v SLS [81,82]. Ultrasound also enhanced the permeability of larger gold nanoparticles (20–40 nm) using ultrasound with a frequency of 3 MHz and intensity of 1.5 W cm^{-2} [83]. Ultrasound has also been used to enable the penetration of peptide dendrimers containing arginine and histidine (as terminal amino acids) with varying positive charges (up to 16$^+$) and up to 2.2 kDa molecular mass [84]. In this research, these dendrimeric peptides were detected in the donor chamber as soon as 10 min post-insonation of human skin (20 kHz, 7–8 W/cm^2 for 30 min), while

passively no dendrimers permeated across human skin after 30 min and only traces were found after 6 h.

The ultrasound conditions used in sonophoresis may vary within the range of frequencies between 0.02 MHz and 16 MHz. The intensity may vary between 0.008 and 50 W/cm^2. The ultrasound intensity is mainly limited in attempt to avoid potential skin damage. Characteristic drug delivery enhancements in drug transport induced by therapeutic ultrasound have been ~10-fold compared to passive drug delivery [85]. This enhancement effect might be appropriate for local delivery of certain drugs (i.e. hydrocortisone) but inappropriate for most drugs. The effect of low-frequency ultrasound (below 100 kHz) on transdermal drug transport has been found to be significantly greater than at higher frequencies (above 100 kHz). For example, Tachibana [46,86] reported that the use of low-frequency ultrasound (48 kHz) yielded greater transport compared to passive transdermal delivery of insulin across diabetic rat's skin. Another example reported by Merino et al. [36] showed that the use of low frequency ultrasound (20 kHz) resulted in greater enhancement of transdermal transport compared to high frequency ultrasound (10 MHz) which did not induce any transport enhancement.

Ueda et al. investigated the cavitational effect of three different ultrasound frequencies (41 kHz, 158 kHz, and 455 kHz) and found that the lower the frequency the greater the cavitation effect. They found that the penetration of calcein across rat skin correlated well with the cavitation generation in the medium, suggesting that indirect effects of cavitation collapse occurring in the insonated medium are more important than their direct effect on the skin [87]. Polat et al. [88] also investigated the effect of ultrasound frequency (20, 40, and 60 kHz) and 1% SLS on the enhancement effect on calcein mass transport across porcine skin. They found that the pore radii created after ultrasound exposure are frequency-dependent on localized transport regions (LTRs, see Section 7). The lower the ultrasound frequency used, the larger the pore radii in LTRs (from 161 Å to more than 300 Å for 60 kHz and 20 kHz, respectively).

Recently, a new way for inducing sonophoresis was investigated and published using two ultrasonic transducers with different frequencies [89,90] simultaneously (Fig. 1). This system utilizes two ultrasound horns perpendicular to each other, one with high frequency (>0.7 MHz) and one with low frequency (typically 20 kHz). The authors claim that the increased sonophoretic effect observed is due to increased generation of cavitational bubbles [91] near the skin from the high ultrasound frequency horn, which in turn can oscillate and collapse when irradiated with the low frequency ultrasound horn, thus synergistically increasing the cavitational effect. Polat et al. [92] used dual frequencies (20 kHz in 50% duty cycle and 1 MHz in continuous mode), intensity of 8.0 W/cm^2 (for the low frequency ultrasound) and 1.5 W/cm^2 (for the high frequency ultrasound) using 1% SLS in 0.01 M PBS as the medium. This apparatus increased the enhancement effect of mass transport of inulin and glucose across porcine skin up to 3.81-fold and 13.6-fold, respectively, compared to single ultrasound frequency. Moreover, Saletes et al. [93] showed that when applying dual ultrasound frequencies instead of a single frequency, a reduction of up to 40% of the intensity may still be sufficient to initiate inertial cavitation. They also found that the greater the difference between the two frequencies the greater the cavitation effect.

The timing of when the ultrasound is used may also play an important role. Basically, two options exist, using ultrasound without permeate and prior to applying it, while the second option uses the ultrasound with the permeate present in the medium. At early studies, simultaneous application of ultrasound and drug was the common approach [73,94]. However, a newer study showed that applying therapeutical ultrasound (1 MHz, 1 W/cm^2) prior to corticosteroid application on human skin results in significant penetration, while simultaneous treatment of ultrasound and corticosteroid doesn't enhance penetration across the human skin in vivo [95]. Shareed and Abdul Rasool tried to develop an optimized sonophoresis protocol for transdermal drug delivery in vitro. They evaluated the effect of ultrasound duration, duty cycle, and the difference between concurrent application of ultrasound and pretreatment with ultrasound. Caffeine was used as the permeate; fixed ultrasound parameters were 20 kHz and intensity of 0.37 W/cm^2. They found that sonication concurrent with permeate deposition was superior to sonication prior to permeate deposition [96].

The use of simultaneous application does provide a temporal control over skin permeability, but it also obligates the patient to use a wearable ultrasound device. Smith [97,98] tried to address this hurdle proposing the use of low-profile light cymbal array ultrasound, which is a flex-tensional transducer (Fig. 2). The cymbal transducer is made of two

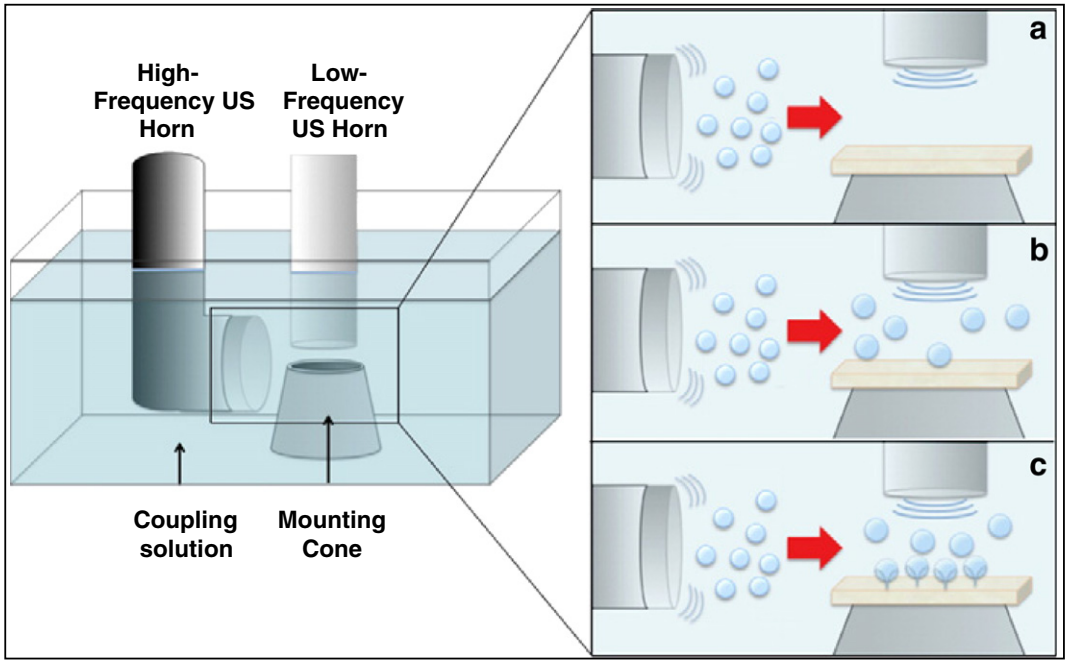

Fig. 1. Schematic diagram of the apparatus using two ultrasonic transducers with different frequencies. It is hypothesized that the high-frequency US horn nucleates small bubbles, which then stream below the low-frequency horn (a). The additional bubbles nucleated by the high-frequency horn grow by rectified diffusion under the influence of the low-frequency horn (b). Upon approaching the skin, the bubbles begin to oscillate non-linearly and collapse toward the skin surface (c) [89].

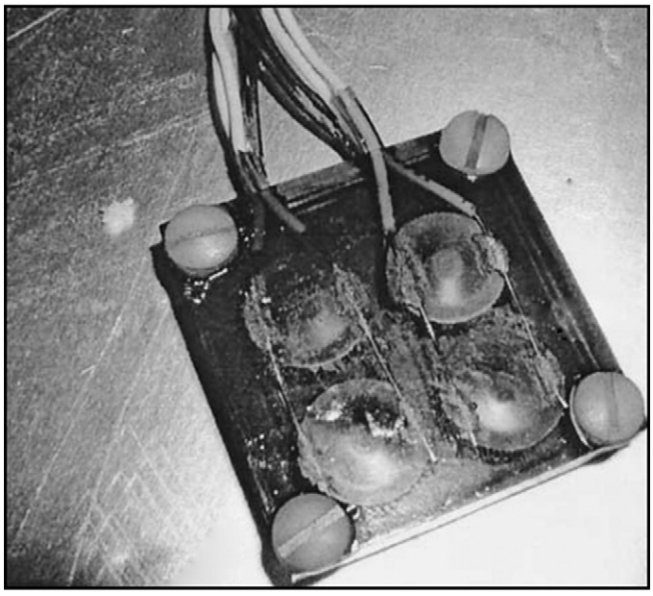

Fig. 2. "Cymbal" array ultrasound device (dimensions 37 × 37 × 7 mm^3). Adapted with permission from [97].

metal caps exposed onto a lead zirconate titanate (PZT) ceramic. Flexing of the end cap is the main mode of vibration. This flexing is induced by the radial motion of the ceramic and the axial motion of the piezoelectric disk. Lee et al. [99] assessed the delivery of insulin to hyperglycemic rats and rabbits using the cymbal array (2 × 2 and 3 × 3 transducers) and ultrasound (37 × 37 × 7 mm^3, 22 g, 20 kHz, and 100 mW/cm^2) [99,100]. The glucose levels of the rats decreased from the baseline (that was set to zero) by 200 and 174 mg/dL for the 5- and 10-minute insonation time groups, respectively (measured 1 h post application). In a more recent study, Park et al. [101] assessed the effect of the cymbal transducer on pigs. The results showed that while for the control group, not exposed to ultrasound, the blood glucose level increased by 31 ± 21 mg/dL (compared to base line value) over the 90-minute experiment, the glucose levels of pigs exposed to 60 min of 20 kHz ultrasound with spatial-peak temporal-peak intensity (ISPTP) of 100 mW/cm^2 showed a decrease by 72 ± 5 mg/dL in 60 min and by 91 ± 23 mg/dL in 90 min, indicating the feasibility of the light weight transducer for human applications. In another study they evaluated the glucose level in rats by noninvasive transdermal insulin delivery using a cymbal transducer array compared with subcutaneously administered insulin (0.15, 0.2, 0.25 U/kg). After the application of ultrasound irradiation for 60 min (20 kHz, ISPTP 100 mW/cm^2, and 20% duty cycle) blood glucose reduced by 262 ± 40 mg/dL within 90 min. On the other hand, when insulin was administered by subcutaneous injection at 0.15 and 0.2 U/kg, little change was observed in glucose level; but for higher concentration of 0.25 U/kg insulin, blood glucose decreased by 190 ± 96 mg/dL within 90 min. The change in blood glucose indicates that a more effective dose of insulin was delivered with ultrasound [102]. Boucaud et al. [103] also demonstrated that after inducing dose-dependent hypoglycemia in hairless rats, exposing them to insulin and ultrasound (energy dose of 900 J/cm^2) resulted in ~75% reduction in their blood glucose levels.

To improve delivery efficiency, a rectangular cymbal design was developed in order to achieve a broader spatial intensity field without increasing the size of the device or the ISPTP [104]. With a similar intensity (50 mW/cm^2), the goal was to determine if the 3 × 1 rectangular cymbal array could perform significantly better than the 3 × 3 circular array for glucose reduction in hyperglycemic rabbits. Rabbit experiments were performed using three groups: non-sonicated control (n = 3), exposed to ultrasound using a circular cymbal array (n = 3), and exposed to ultrasound using a rectangular cymbal array (n = 3). Rabbits were anesthetized and a water-tight reservoir that held the insulin was fastened on the rabbit's thigh. At the beginning of the experiment and every 15 min for 90 min, the blood glucose level was determined. For the control group, the normalized glucose level increased (more hyperglycemic) by 80.0 ± 28.8 mg/dL (mean ± SEM). Using the circular array, the glucose level decreased by 146.7 ± 17.8 mg/dL from the base level after 90 min. However, using the rectangular cymbal array, the glucose decreased faster and by 200.8 ± 5.9 mg/dL after 90 min (below the baseline concentration that was set to zero). These results indicated the feasibility of the rectangular cymbal array as an improved device for drug delivery.

Mitragotri and Kost also tried to address the issue of using a wearable ultrasound device [66,68]; they proposed an approach in which ultrasound was applied briefly as a pretreatment process followed by passive diffusion, therefore rendering the need for wearable device. Other studies have also reported the use of the pretreatment-type sonophoresis. However, this approach possesses a challenge, requiring the determination of the degree of skin permeabilization prior to drug placement [105].

Insulin uptake through the skin increased after pretreatment with low-frequency ultrasound (20 kHz, ~7 W/cm^2). Rat's skin conductivity increased approximately 60-fold post insonation. In these experiments, insulin (500 U/mL) was applied to rats' skin after ultrasound treatment, which caused their blood glucose concentration to decrease by approximately 80% within 2 h [106]. However, blood glucose concentration remained unchanged when insulin was applied on untreated skin. Low molecular weight heparin (LMWH) transport across rats' skin in vivo was also assessed with and without ultrasound pretreatment [77]. Anti-Xa (aXa—a plasma factor in the coagulation cascade) activity in blood was used for the assessment of transdermal LMWH delivery. No significant change in aXa activity was observed when LMWH was applied to non-treated skin. However, a significant quantity of LMWH was detected that has been transported transdermally when applied after insonation pretreatment. The activity of aXa in the blood was found to increase slowly for about 2 h post insonation. Subsequently it increased rapidly reaching a steady state after 4 h at a value of about 2 U/mL [77] as opposed to what was achieved with intravenous or subcutaneous injections (which resulted only in transient biological activity). The effect of transdermal delivery of LMWH with ultrasound pretreatment was observed well beyond 6 h.

Another example for macromolecular transport was shown by Katz et al. [65]. They also applied ultrasound (55 kHz) as a pretreatment to shorten the lag-time for the analgesic agent EMLA® cream (AstraZeneca International, Wilmslow, UK) to become effective. EMLA cream contains two local anesthetics (lignocaine and prilocaine). It is designated to induce local analgesia for normal intact skin for about 1 h post application. Forty-two human subjects participated in the study in which pain scores were measured and patients' preferences recorded. Pain scores and overall preferences recorded after 4–14 s of ultrasound pretreatment followed by EMLA cream application 5, 10, and 15 min later, were statistically indistinguishable from EMLA cream application for 60 min without ultrasound pretreatment.

The gel composition also plays a role in skin permeation enhancement as was shown by Mishali et al. [107]. Ibuprofen transport across rabbit skin increased with alcohol concentration in the gel and decreased with the addition of propylene glycol (without the use of ultrasound). The combined application of ultrasound and gel further increased the transport of ibuprofen, but as previously explained, ultrasound-induced cavitation phenomena decrease with increasing gel viscosity, and this should also be taken into account when attempting to optimize the ultrasound effect.

The effectiveness and clinical use of sonophoresis were studied by Becker et al. [108,109]. Eighty-seven patients joined the study. A brief (15 s) ultrasound exposure was applied as a pretreatment (similar to Katz et al. [65] using the SonoPrep®), followed by 5 min application of 4% liposomal lidocaine cream and standard care intravenous

cannulation. Patients reported significant reduction in perception of the pain of intravenous cannulation. Also, none of the patients reported any adverse side effects during the follow-up period. Based on these and additional studies the U.S. Food and Drug Administration (FDA) granted a 510 k marketing clearance to Sontra Medical in August 2004 to market the SonoPrep® ultrasonic skin permeation device and procedure tray for use with topical lidocaine. SonoPrep® (Fig. 3) was evaluated by Prausnitz et al. in 2009 for its ability to induce long-term effects on human skin. They found that after exposing the forearm skin of adults to SonoPrep® at a frequency of 55 kHz, intensity of 15 W/cm^2 until the skin was permeabilized, the occluded exposed area is highly permeable for 42 h post-exposure in a reversible manner [110]. Krishnan et al. [111] also found that applying SonoPrep® onto human skin enabled the penetration of 5-Aminolevulinate (used for actinic keratosis and other non-melanoma skin cancers), whereas in untreated skin it did not penetrate the skin at all. The SonoPrep® induced a flux of 5-Aminolevulinate of 54.8 ± 8.0 μg/cm^2 h.

For other approved ultrasound devices we refer the readers to reviews by Mitragotri and Sing et al. [112,113]. For a brief review on industrial and commercial aspects of developing therapeutic ultrasound see Seip [114].

3.1. The relationship between mass transport, skin resistivity and water uptake

The relationship between DC current and voltage and sodium ion transport for human allograft skin immersed in saline buffers has been studied by [115]. Most of their samples yielded sodium ion permeability coefficients less than or equal to those reported for human skin in vivo. The current–voltage relationship in these tissues was time dependent, highly nonlinear, and slightly asymmetric with respect to the sign of the applied potential. Skin resistance decreased as current or voltage increased. This decrease was almost completely reversible for current densities less than 15 μA/cm^2 and exposure times of 10–20 min. At higher current densities, both reversible and irreversible effects were observed. The overall dependence of current (I) on voltage (V) was nearly exponential and was satisfactorily described by I ~ sinh(V). At a current density of 71 μA/cm^2 and transmembrane potentials 1.1–1.6 V the flux enhancement for sodium ion was three to five times larger than that predicted for an uncharged homogeneous membrane according to electrodiffusion theory.

Fig. 3. 2nd generation SonoPrep® device.

The relationship between skin electrical conductance (and resistance) and skin permeability has been formally established [116]. It has been shown that the skin's conductance correlates well with its permeability irrespective of the means by which the permeability is enhanced. Karande et al. used electrical conductance measurements to assess the effect of chemical penetration enhancers on skin permeability [117]. Skin conductance is measured continuously during in vitro, in vivo, or in clinical experiments determining the needed ultrasound application time. Ultrasound insonation time depends on the objectives of the experiment. In the past, a predetermined value of conductance was set and once the skin reached that value the insonation stopped [65]. A more recent method uses a feedback control loop in which the change in conductance is calculated online using the second derivative of the typical sigmoidal graph representing the change in conductance with insonation time [105,108–110,118].

In a later study, White et al. (2011) analyzed single-frequency LCR databridge impedance measurements to determine whether the barrier of skin samples has sufficient integrity for meaningful measurements of in-vitro chemical permeability [57]. Tritiated water permeation has been a conventional skin integrity test, however steady state determination of tritiated water permeability, based on water flux measurements may require over 2 h. Single-frequency electrical impedance measurements are rapid and economical alternatives to tritiated water flux measurements. The method involves measuring the potential or current response to a small-amplitude, typically sinusoidal modulation of an input current or potential. Previously skin integrity has been assessed by LCR databridge measurements, which were reported as resistances determined in either series (SER) or parallel (PAR) modes at a single frequency, typically 100 or 1000 Hz. It has been previously noted that measurements made at different combinations of mode and frequency differed. White et al. [57] provided a theoretical interpretation of these differences and their impact on the skin integrity test results and experimentally confirmed their theoretical findings. SER mode resistances are equal to the real part of the admittance—the multiplicative inverse of the complex impedance. Capacitance measurements reported in SER and PAR modes are similar manipulations of the imaginary parts of the complex impedance and admittance. They used a large amount of data from human cadaver skin to show that PAR-mode resistance and SER-mode capacitance measured at 100 Hz are sensitive to skin resistivity, which is the electrical measurement most closely related to skin integrity.

The skin impedance is the alternating-current analog of the area-normalized resistance under DC-current, R_{skin}. It is the complex ratio of the voltage to the current in an alternating current whose argument f equals the phase difference between them. As f approaches zero the skin impedance approaches R_{skin} and the real part of its multiplicative inverse—the conductance approaches a value proportional to the water permeability. The skin electrical resistivity, ρ quantitatively characterizes the pathway for ionic transport through a skin area of A. It satisfies $\rho = \delta^{-1}(R_{skin}A)$, where δ is the thickness of the skin layer primarily responsible for the electrical resistance, commonly the stratum corneum (10–40 μm) [57]. The permeability of polar and ionic chemicals through the skin has been shown to be proportional to $(R_{skin}A)^{-1}$. Denoting the permeability coefficient of an ionic compound *i* by P_i, it can be shown that

$$b_i = \frac{P_i}{(\rho\delta)^{-1}} = P_i(R_{skin}A) \tag{2}$$

where b_i ($=b_i$ (f)) is the compound-specific proportionality coefficient of the ionic compound *i*.

While the impedance measured at low frequencies may provide a good estimate of R_{skin} and thus be inversely proportional to the permeability coefficient of polar and ionic compounds. Alvarez-Roman et al. suggested that the increase in skin permeability after ultrasound

application, manifested by increased skin conductivity, is due to SC's lipid extraction, which was found to be approximately 30% [119].

4. Immunization using ultrasound

Transcutaneous immunization is a procedure in which vaccine antigens in a solution are applied on the skin to induce an antibody response without systemic or local toxicity [120]. The major advantage of transcutaneous immunization is the presentation of immunogens to antigen presenting cells (APCs) within the skin, specifically Langerhans cells that are highly potent immune cells within the epidermis. Langerhans cells are in close proximity to the outermost layer of the skin, the SC, and represent a network of immune cells that occupy about 20% of the skin's total surface area despite composing only 1% of the epidermis cell population [121]. Langerhans cells initiate immune responses by acting as professional APCs, taking up and processing antigens, and subsequently presenting antigenic peptides to naive T-cells in the lymph nodes [122,123]. Transcutaneous immunization has been shown to generate both systemic (IgG/IgM response) and mucosal (IgA response) immunity, whereas conventional needle-based injections often only generate systemic immunity [120,124,125].

Tezel et al. [67] have demonstrated that ultrasound as a pretreatment (20 kHz, 100 J/cm^2) induces a significant IgG response and activation of Langerhans cells in the epidermis to a model vaccine (tetanus toxoid) in BALB/c mice. The authors also demonstrated that low frequency ultrasound acts as a transcutaneous immunization adjuvant that abolishes the requirement of toxins to elicit an immune response. Ten microgram of subcutaneous injection of tetanus toxoid induced an immune response comparable to the delivery of as little as 1.3 μg of tetanus toxoid by low-frequency ultrasound. Murdan et al. [126] showed that in the absence of sodium lauryl sulfate (SLS), tetanus toxoid delivery to skin pre-treated with low frequency ultrasound resulted in anti-tetanus toxoid IgG and neutralizing antibody titers that were above those required for protection against tetanus. This indicates that SLS may not be required for low frequency sonophoresis (LFS)-assisted transcutaneous immunization. In addition, they showed an inverse relation between SLS concentration and antibody titers; low concentration of SLS increases the antibody titers, and low ultrasound duty cycle (10 or 20%) increases the generation of IgG and neutralizing antibody titers. This indicates that enhancement of skin permeability is not the main mechanism of LFS-assisted skin immunization [126]. In another study they showed that using liposomes as a vaccine adjuvant reduced antigen permeation and trans-epidermal water loss (TEWL) when the skin was pre-treated with LFS using phosphate buffer solution (PBS) as a coupling medium. On the other hand, such skin repair did not take place in the presence of SDS and no changes were noticed in antigen permeation and TEWL. Moreover, they found that skin repair is more effective with smaller liposomes and it depends on the extent of the disruption caused by the ultrasound [127].

5. Gene therapy

The concept of enhanced topical gene therapy with the aid of ultrasound seems promising [128–131]. Gene therapy is a method for amending defective genes that are accountable for disease development, usually by substituting an “abnormal” disease-causing gene with the “normal” gene. The therapeutic gene is typically delivered to the targeted cell/organ (or systemic circulation) with the use of a carrier molecule (vector). The progress made in genome research that resulted in the discovery of almost 100 defected genes causing skin related diseases, has made the possibility of using gene therapy a promising option [125,132–136]. Several of these studies (i.e., diabetic ulcers and peripheral ischemic ulcers) have reached the stage of clinical trials [137,138]. Severe forms of genodermatoses (monogenic skin disorders) such as epidermolysis bullosa and ichthyosis [131,139,140] are obviously the best candidates to be addressed by cutaneous gene therapy. Tran et al. showed that insonating melanocytic lesions followed by topical treatment of liposomal-siRNA complex (targeting ^{V600E}B-Raf gene) significantly decreased (~30–40%) cutaneous tumor development in animals [141]. Other applications may be used for immunization, wound healing, vitiligo, melanoma, atomic dermatitis, and psoriasis (for details on these applications see [142]).

Topical gene therapy necessitates the permeation of a large complex to or across the skin. The vector–gene complex can enable these required features via ultrasound pretreatment of the skin due to the ultrasound enhancing effect on skin's permeability. Although the main challenge in topical gene delivery remains overcoming the skin and cells' uptake barrier, only few researchers have utilized ultrasound (or any other mechanical method) for this purpose; it is believed that improved delivery and dermal cell uptake can be achieved by this method.

It is important to mention that ultrasound has been used extensively for enhancing uptake into cell lines and overcoming transfection barriers. Since it is out of the scope of this review, interested readers are encouraged to read the article of Prausnitz et al. regarding this issue [143].

6. Transdermal monitoring using ultrasound

Extensive efforts have been devoted to developing painless and convenient techniques to measure blood analytes, particularly glucose. These techniques include implantable sensors, minimally invasive skin microporation, methods involving laser or miniaturized lancets. It also includes noninvasive approaches such as near-infrared spectroscopy, chemical penetration enhancers, and reverse iontophoresis [144]. One of the crucial problems in noninvasive transdermal diagnostics is obtaining adequate quantities of analyte for detection. Ultrasound, particularly at low frequencies, has been shown to have an enhancing effect on skin's permeability, hence allowing adequate quantities of clinically relevant analytes, including glucose, to be collected for noninvasive monitoring [66,118,145].

The technique was evaluated on type 1 diabetic patients to assess whether a single short insonation (less than 2 min) was adequate to noninvasively extract sufficient quantities of glucose across human skin for several hours, and to determine whether transdermal glucose flux varied in response to variations in blood glucose levels. Additional experiments to further evaluate the duration of ultrasound-induced permeability found that the skin permeability remained high for about 15 h and returned to its normal value by 24 h [66]. Venous blood glucose concentrations and noninvasively extracted glucose fluxes after insonation as a pretreatment were in good correlation. Variations in skin permeability of different sites after insonation were tested for the same patient and among patients. The inconsistency in site-to-site permeability was found to be approximately the same as patient-to-patient variability. This necessitates a one-point calibration between transdermal glucose flux and one blood sample, which in turn is used to forecast subsequent blood glucose levels. Based on such a calibration, the relationship was evaluated between transdermal glucose flux and blood glucose levels (17% mean relative error). Echo Therapeutics Inc. [99] has developed this technique for noninvasive continuous detection of glucose. A minimally invasive method that continuously measures glucose flux across insonated skin was reported [145]. In this study the glucose concentrations of ten diabetes patients were examined over a period of 12 h, and 8 patients undergoing cardiac surgery were monitored for 24 h. The transdermal continuous glucose monitors usually required 1 h of warm up. Depending on the study setting, single or multiple calibrations were applied, demonstrating successful accuracy of glucose prediction in these diverse clinical settings.

Lee et al. [99] demonstrated the prospect for quantifying glucose levels in interstitial fluids (ISF) after enhancement of skin permeability with a light cymbal ultrasound array (37 × 37 × 7 mm, 22 g, 20 kHz). A total of 12 anesthetized rats were divided in two groups (US exposure group and control group). The ultrasonic transducer array with a saline

reservoir (ISPTP = 100 mW/cm^2) was affixed to the abdomen. The array was removed after 20 min of exposure and an electrochemical glucose sensor was placed on the exposed area to determine the glucose concentrations through the skin. The externally measured concentrations were in good correlation with blood glucose levels measured in blood tests.

In an attempt to improve the accuracy of continuous glucose monitoring systems, Jin et al. used skin impedance measurement to monitor the skin permeability variation. They used low frequency ultrasound to enhance the skin permeability by disrupting the bilayers of the SC and ISF extracted by vacuum. The concentration of glucose was predicted by a biosensor from extracted ISF. They measured the skin impedance and transformed it to skin conductivity for estimating the correlation coefficient between skin permeability and conductivity. They claimed that using this method improved the prediction accuracy of the continuous blood glucose monitoring system [146].

Park et al., in their study, used a combined ultrasound system of insulin delivery and glucose sensing by a feedback controller. The in vivo experiments were performed on 200 lb pigs. They used a cymbal ultrasound array (3 × 3, 30 kHz, ISPTP = 100 mW/cm^2) for insulin delivery and (2 × 2, 20 kHz, ISPTP = 100 mW/cm^2) for glucose sensing. For their experiments 115 mg/dL was set as reference value for operating the combined system, which delivers insulin automatically based on glucose blood level. The glucose levels were determined every 20 min for 2 h. They found that glucose levels determined by their system were slightly higher in comparison with a commercial glucose meter. They suggested that in view of the in vivo results, using a feedback-controlled combined cymbal ultrasound array system for noninvasive glucose sensing and insulin delivery is feasible [147].

7. Mechanism

In the past three decades, the mechanism of the sonophoresis phenomena has been studied. Although many studies have been published on the subject, the mechanism is still not fully understood. What is known is that the main ultrasonic effects are: cavitation, acoustic streaming, thermal effects, and recently the BLS. However, it has been shown in most cases that inertial cavitation is the main effect responsible for enhanced transdermal mass transport. All recent studies point out that cavitation plays a significant role in the enhancing mechanism of ultrasound treatment. For example, Mitragotri et al. [48] assessed the role of a number of ultrasound-related phenomena, including cavitation, thermal effects, generation of convective flows, and mechanical effects. The authors theorized that the enhanced transdermal transport in the course of low-frequency ultrasound application occurs through the keratinocytes rather than the hair follicles. They proposed that cavitation generates disorder of the SC lipids, causing significant water penetration into the disordered lipid region. This might prompt the formation of aqueous channels through the intercellular lipids of the SC enabling the transport of permeates.

Some attempts have been made to establish an appropriate mathematical model (see Section 8) that could describe the enhancement in transport phenomenon and predict the enhancement factor for various drugs at various settings [116,148–150]. Tezel and Mitragotri [71] presented a theoretical analysis of the interaction of SC lipid bilayers with cavitation bubbles. Three scenarios were considered—shock-wave emission, micro-jet penetration into the SC, and impact of micro-jet on the SC (see Fig. 4 for the first two scenarios). Their model predicts that both micro-jets and spherical collapses might be accountable for the observed transport enhancement effect. Ueda et al. examined the cavitational effect of three ultrasound frequencies (41 kHz, 158 kHz, and 455 kHz) and found that the lower the frequency used, the greater the cavitation effect. They also found that the penetration of calcein across rat skin correlated well with the cavitation generation in the medium, suggesting that indirect effects of bubble collapse that occur in the insonated medium are more important than the direct action on the skin [87].

Additional potential mechanism of improved percutaneous transport post insonation was suggested by quite a few groups [45,148,151], hypothesizing that ultrasound interacts with the structural lipids situated in the intercellular channels of the SC. This is similar to the assumed effects of some chemical penetration enhancers that mainly act by disarranging lipid structures either by extracting lipids from the bilayer or by penetrating it [152]. Tachibana [46] and Simonin [148] hypothesized that the energy of ultrasonic vibration induces enhanced transdermal mass transport via the trans-follicular and trans-epidermal routes. They proposed that microscopic bubbles (cavitation) formed at the surface of the skin by ultrasonic vibration might produce a rapid liquid flow, thus increasing skin permeability.

Wolloch and Kost investigated the importance of micro-jets versus shock waves in cavitation formation [153]. They found that micro-jets created by bubble collapse (inertial cavitation) are significantly more effective in increasing skin permeability compared to shock waves. They showed that micro-jet formation is increased when adding large particles (250 μm) to the solution, whereas adding small particles (10 μm) increases the formation of shock waves that act as suppressors

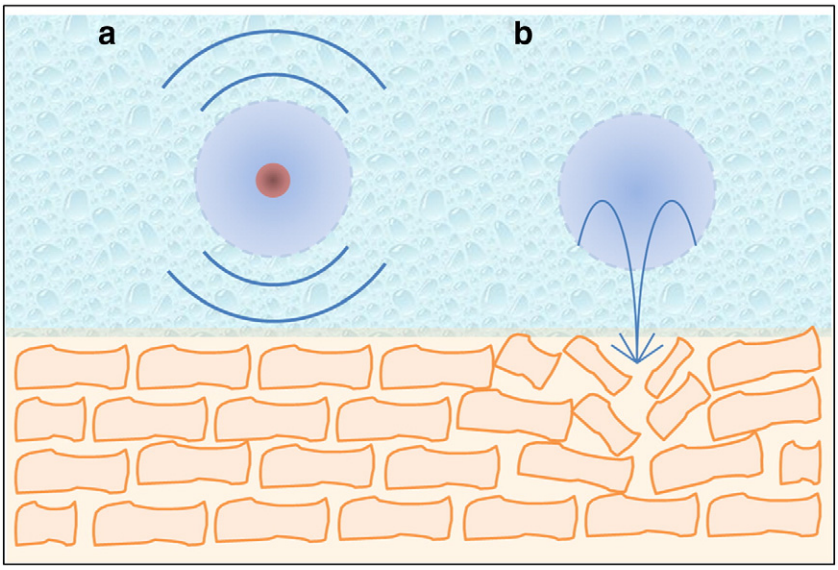

Fig. 4. Main bubble collapse scenarios; (a) shock waves, and (b) micro jets.

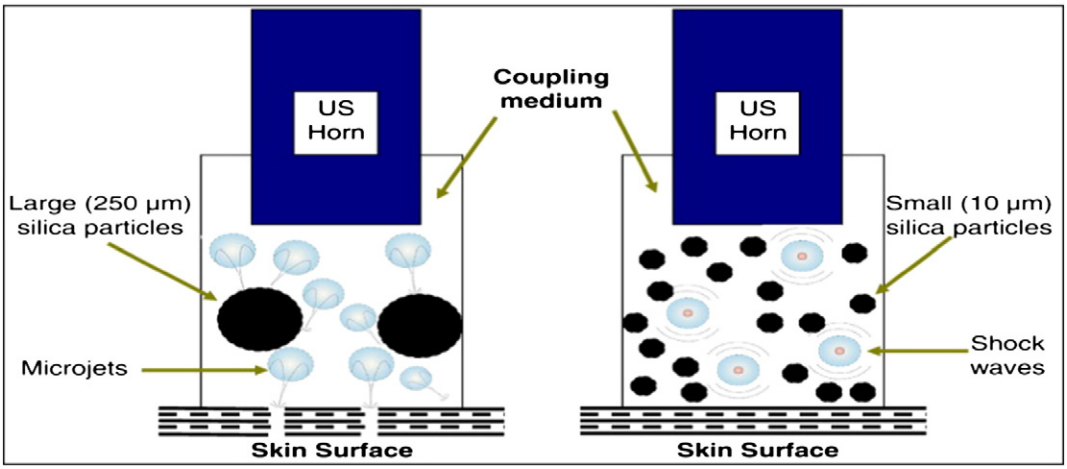

Fig. 5. The addition of silica particles to insonated medium: the particle size effect on the formation of micro jets and shockwaves [152].

for micro-jet formation near the skin surface (Fig. 5). This finding should be taken into account for researchers who seek to use ultrasound with carriers (either for drugs or genes).

Significant efforts have been focused on understanding the permeation pathways through the skin during low-frequency sonophoresis [15]. The effects of ultrasound-induced cavitation on skin have been shown to be highly heterogeneous, leading to localized regions of high permeability [153–162]. Kushner et al. [155] demonstrated that the localized transport regions (LTRs) are approximately 80-fold more permeable than the surrounding regions of the skin (see Fig. 6 for images of LTR formation). The transport was enhanced in response to ultrasound irradiation even in the non-LTR regions. Specifically, the skin electrical resistivity of the non-LTRs was found to be approximately 170-fold lower than that of untreated skin, while the electrical resistivity of the LTRs was found to be approximately 5000-fold lower than that of untreated skin. It was also found that the LTRs obtained with higher ultrasound frequencies were more homogeneously distributed in the skin [154]. Optimal LTRs with significant transport enhancements were obtained around 60 kHz. These results suggest that the difference in the permeabilities of the LTRs and non-LTRs is due to the creation of more aqueous channels in the LTRs than in the non-LTRs [49,158]. The authors confirmed the presence of LTRs using two-photon microscopy [156]. This conclusion of Kushner et al. can be further assured from the results of Polat et al. [51], who found that ultrasound induces new pores in LTRs and that the pore radius (>300 Å) is significantly larger than in untreated ("native") porcine skin (~13.6 Å). See more details on this research in Section 10.

Alvarez-Román et al. [119] studied the effect of insonation (20 kHz) on skin using confocal microscopy. They reported that the permeabilized areas of skin by sonophoresis were discrete and were separated by regions of the SC that had not been significantly affected by the application of ultrasound. In some regions, profound accumulation of permeated fluorophore was seen below the SC; however, adjacent sites in ultrasound-treated skin showed that there was retention of the fluorescent probe at the SC surface and, by implication, no opening of new permeation pathways across the barrier. The distribution and number of LTRs in the skin changed with the frequency of ultrasonic exposure.

Paliwal et al. [160] studied the heterogeneity of transdermal transport during sonophoresis using quantum dots (QDs, 20 nm in diameter) as tracer nanoparticles. Microscopically, QDs were captured in several discrete pockets, each spanning about 40–80 μm in width and up to 60 μm in depth in the LTRs, and were shown to penetrate into the viable layers of the skin. A high heterogeneity in QD distribution was also observed at the nanometer length-scale in the skin using electron microscopy. Existence of QD-localized pockets (up to 50 nm wide and 300 nm long) was observed within the intercellular lipids and corneodesmosome junctions of the SC, and occasionally in corneocytes of the LTRs. Electron micrographs of untreated skin showed scattered and non-connected defects within the intercellular lipid lamellae, while application of ultrasound (20 kHz, 2.4 W/cm^2) significantly increased the frequency of occurrence as well as the size of defects in the bilayers of the SC. Furthermore, application of ultrasound in the presence of SLS induced similar but more pronounced dilatory defects in the ultrastructure of the SC. Quantitative analysis showed that while the area-density of defects significantly increased in the SC, their number-density did not change for ultrasound-treated skin compared to controls. The authors hypothesized that ultrasound induces dilatation and greater connectivity of voids in the SC, which possibly leads

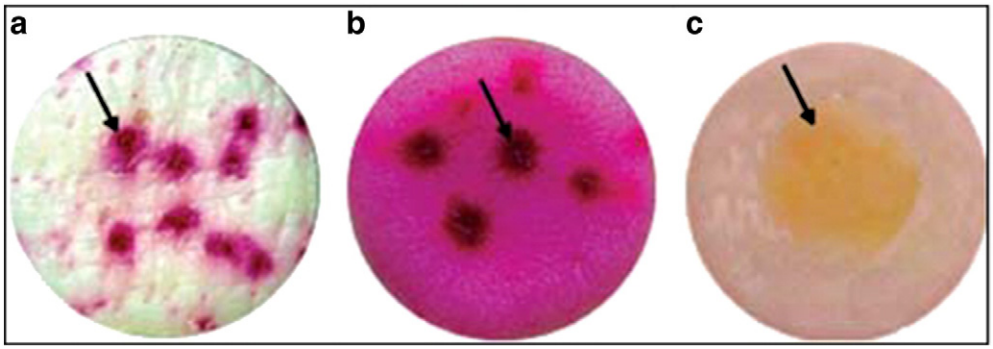

Fig. 6. Representative images of LTR formation in: (a) full-thickness pig skin with sulforhodamine B (SRB), (b) full-thickness human cadaver skin with SRB, and (c) full-thickness hairless rat skin with fluorescein isothiocyanate dextran (FITC-dextran 40). In (a)–(c), the black arrow points to a representative LTR in each skin sample [154].

to the formation of a well-connected three-dimensional porous network in the SC, which is capable of transporting QDs as well as other macromolecules across the skin.

A very interesting article published in 2009 by Collis et al. [163] may offer an explanation for why LTRs are formed after ultrasound application. They investigated the differences in the shear stresses created by cavitational bubbles depending on their size (as a result of using different ultrasound frequencies). They analyzed three different shear stress patterns (termed quadrupole, dipole, and vortex, Fig. 7) with increasing flow field divergence that may develop near surfaces such as skin or cell membranes. They found that surface divergence affects the developing flow field, thus affecting different parts of the tissue/cell different flow fields, causing stretching/opening in some zones but contraction in others (one should also bear in mind that ultrasound cavitation results in a variety of bubble radii). This may also be used in studies evaluating the effect of ultrasound on cell permeability as to why not all cells experience the same effect when exposed to ultrasound.

Tang et al. [149] evaluated the relative roles of enhanced permeability due to ultrasound-induced skin alteration and enhancement due to ultrasound-forced convection. The theoretical and experimental results propose that, for low-frequency ultrasound, the relative influence on enhanced diffusion depends on the in vitro skin model used. Specifically, convection plays a central role when heat-stripped SC is insonated, while its effect is minimal when full-thickness skin is employed. Also, the actual pore radius of the skin calculated using heat-stripped SC in the course of ultrasound exposure is much larger than that within full-thickness skin.

As mentioned previously, it is generally agreed that skin electrical conductivity is proportional to skin permeability, either may be used to represent the other [57,162,164–166]. The normalized model simulation results were compared to measured electrical conductivity for various experimental scenarios. The model predicts realistic characteristic times observed in sonophoresis (10 s to 5 min). The computational predictions qualitatively conform to the experimental results. Sonophoresis may result from various mechanisms that act in synergy. The present model predicts that rectified diffusion (see Section 8 for further details) might be one of the factors that lead to sonophoresis during ultrasound treatment.

Morimoto et al. [167] studied the transport pathway of fluorescent-labeled hydrophilic dextran molecules (40 kDa) in hairless rat skin after low-frequency sonophoresis using confocal microscopy. Upon ultrasound exposure (41 kHz, 120 mW/cm^2, 5 min), dextran molecules penetrated into the skin up to a depth of 20 μm. Several crack-like structures were observed in the sonicated skin that lay under the ultrasonic transducer. On the other hand, when using Rhodamine B the penetration depth was about the same as with passive diffusion, although there was an increase in the quantity penetrating to each layer depth investigated. The authors believe that the different transport patterns of dextran and Rhodamine B may be due to differences in their lipophilicity. Because the ultrasound increases water transport across the skin, distribution of more lipophilic compounds such as Rhodamine B may not be influenced significantly as opposed to FITC dextran, which is hydrophilic. The authors concluded that ultrasound increased the transdermal transport of hydrophilic solutes by causing a degree of structural alteration and then inducing convective solvent flow probably via both corneocytes and lipids of the SC. Kushner et al. [156] also investigated the depth penetration of Rhodamine B hexyl ester (RBHE, hydrophobic permeant) and sulforhodamine B (SRB, hydrophilic permeant) using dual channel two photon microscopy. The results showed that RBHE and SRB both penetrated the skin up to 40 μm after ultrasound application (in LTR regions). Lanke et al. used SonoPrep® (55 kHz for 1 min) and 0.1% SLS for assessing the penetration depth of LMWH, and found that LMWH penetrated insonated skin up to 100 μm compared to 40 μm in passive diffusion [168]. The increase in depth penetration is due to the addition of SLS to the medium interfacing with the skin since it is known to interact synergistically with chemical penetration enhancers [92].

8. Models and simulations

The enhanced transdermal drug delivery under the influence of ultrasound (US) irradiation, termed sonophoresis, has been studied extensively in the past – experimentally as well as theoretically – yet it is in many aspects controversial and actually many details remain poorly understood. Mathematical models are used to formulate hypotheses in terms of equations and parameters and their solutions provide theoretical basis and insight of the observed phenomena.

The most prominent phenomena associated with ultrasound irradiation are the creation of gas bubbles from small gas nuclei in the ambient medium and their rapid oscillation. If the ambient pressure is not too large, these bubbles grow due to the *rectified diffusion* phenomenon: gas enters and exits the bubbles by diffusion under the oscillating pressure. It enters the bubble during the pressure rarefaction expansion phase and exits during the compression phase. The quantity of air transported in each phase is proportional to the bubble surface area. The surface area during the expansion phase exceeds the surface area during the compression phase. Consequently, over a complete cycle, there will be a net increase in the quantity of gas in the bubble, a phenomenon called rectified diffusion.

Bubbles that reach an unstable diameter collapse symmetrically when surrounded by an infinite medium and asymmetrically near a wall. The bubble boundary farthest from the wall moves towards the wall, sometimes penetrating the boundary nearest to the wall, thus, creating micro-jet that impinges the skin surface. Symmetrically collapsing bubbles induce shockwaves. Bubble oscillation, growth, and collapse under the influence of an ultrasonic field are termed acoustic cavitation.

Here we attempt to provide an overview of the most prominent mathematical models that have been used to describe the LFS-enhanced

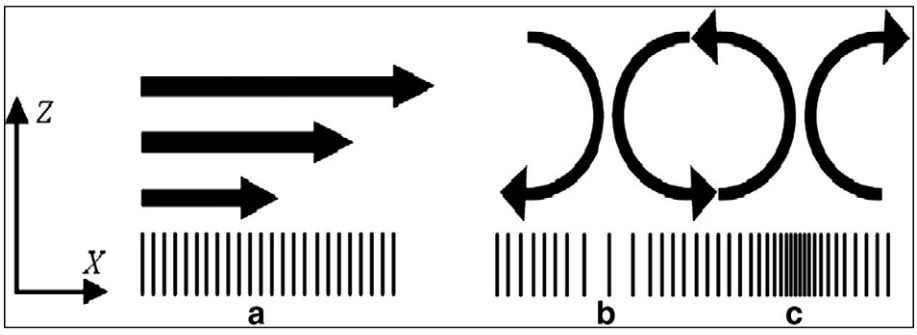

Fig. 7. Illustration of the difference between uniform shear and surface divergence; (a) uniform, high shear stress, no divergence and hence no stretch of cell surface; (b) high rate of positive divergence (as well as shear stress), cells/cell membrane in stretch-activated state; (c) high rate of negative divergence (as well as shear stress), cells/cell membrane compressed together.
Adapted with permission from [162].

transdermal drug delivery. Mathematical models can be categorized according to various criteria. Clearly, various ultrasound-related phenomena, including cavitation, thermal effects, convective velocities, and mechanical effects can affect the enhanced transdermal drug delivery (TDD). Here, the mathematical models will be presented according to the mechanism that is assumed to dominate observed experimental data. The following categories will be considered with regard to the dominating factor in LFS-enhanced TDD:

1) Enhanced diffusion due to US-induced structural alterations—in the late 1960s and early 1970s, Blank and Scheuplein applied the quantitative-structure permeability relation (QSPR) approach [169]. QSPR methods link SC permeability to the permeant partition coefficient, its diffusivity, and the SC thickness based on the assumption that permeant transport through the SC is done by Fickian diffusion. The SC is treated as a uniform, lumped membrane. QSPR methods use statistical correlations to express the permeability coefficient under normal, undisturbed conditions and following structural changes.
   Mitragotri et al. in 1995 [151] hypothesized that oscillations of the ultrasound-induced cavitation bubbles near the SC keratinocyte-lipid bilayer interfaces may cause oscillations in the lipid bilayers, thereby causing structural disorder of the SC lipids. They speculated that shock waves generated by the bubble collapse may further add to the structure-disordering effect. They proposed a QSPR-based mathematical model for the undisturbed, passive skin permeability coefficient as a function of the partition coefficient of the permeant in the bilayer, the effective permeant diffusion coefficient, and the thickness of the SC.
   Similarly, they described the effective electrical conductivity of the skin based on the transport of ions such as sodium and chloride (present in the saline solution around the skin) through the shunt pathways as well as through intercellular lipids. Next they presented a mathematical expression for the skin permeability coefficient for permeates in the presence of US and a corresponding description of the electrical conductance of the skin. Dividing the latter expressions by the former ones produced the enhancement ratios of permeability and electrical conductivity in the presence of US. These models suggest that the transport rates of drugs passively diffusing through the skin at low rate are most enhanced by the application of US.
2) Porous pathway models—Tang et al. [149] in 2001 suggested a different mechanism. They hypothesized that the TDD enhancement may result from US-induced skin alterations and/or from forced convection. They began by developing a theory describing the transdermal transport of hydrophilic permeates in both the absence and the presence of US, incorporating fundamental equations of membrane theory and electrochemistry principles.
   A fundamental assumption in their model is that hydrophilic permeants migrate through the skin via a porous pathway, which is the same pathway traversed by current-carrying ions. Further assumptions in their model include: 1) the permeant/ions behave as hard spheres with no specific interactions with the pore walls, and 2) the anions and cations in the electrolyte solution have the same valence and similar transport characteristics. In a later study, Tezel et al. [164] in 2002 modified the previous model to include lipophilic pathways as well.
3) Intercellular-cavitation—Lavon et al. in 2007 [150] presented a simplified model of a process based on rectified diffusion that could lead to channeling and thereby to transdermal sonophoresis (Fig. 8). According to their model, small gas bubbles randomly distributed in the lipid bilayers of the SC grow in the presence of US by rectified diffusion. These bubbles may merge and create elongated gas channels that propagate along the lipid bilayers. As they reach the boundaries of the SC they fill with water, through which drugs can easily penetrate. Partially or fully opened channels shorten the diffusion path and as a result transdermal transport is enhanced. Equivalently, these channels also reduce the electrical resistance between the outer and inner surfaces of the SC. Their resultant resistance can be calculated by treating them as electrical/diffusional resistors connected in parallel. Neglecting their tortuosity, their electrical as well as diffusional conductance can be roughly related to their length relative to the SC thickness. Eller's equations were applied

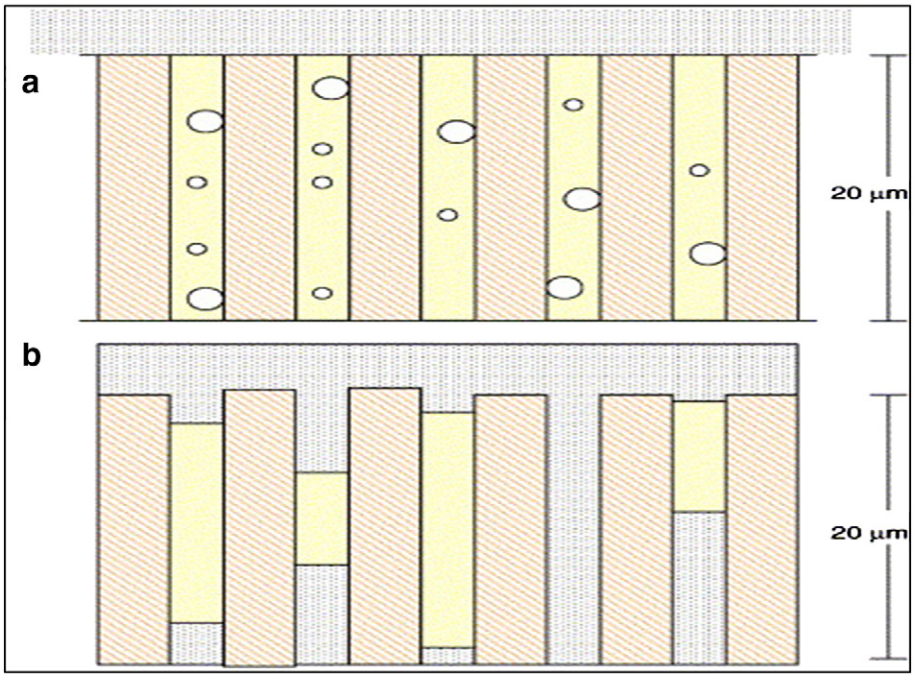

Fig. 8. Schematic representation of model scenario: (a) Initial state: small gas bubbles are randomly distributed within channels present in the lipid matter of the SC. (b) Final state: termination of rectified diffusion process. When no bubbles are left, the process reaches an endpoint, and is terminated. Some channels are fully opened. Other channels are partially opened. Keratinocytes; lipid matter; aqueous medium [149].

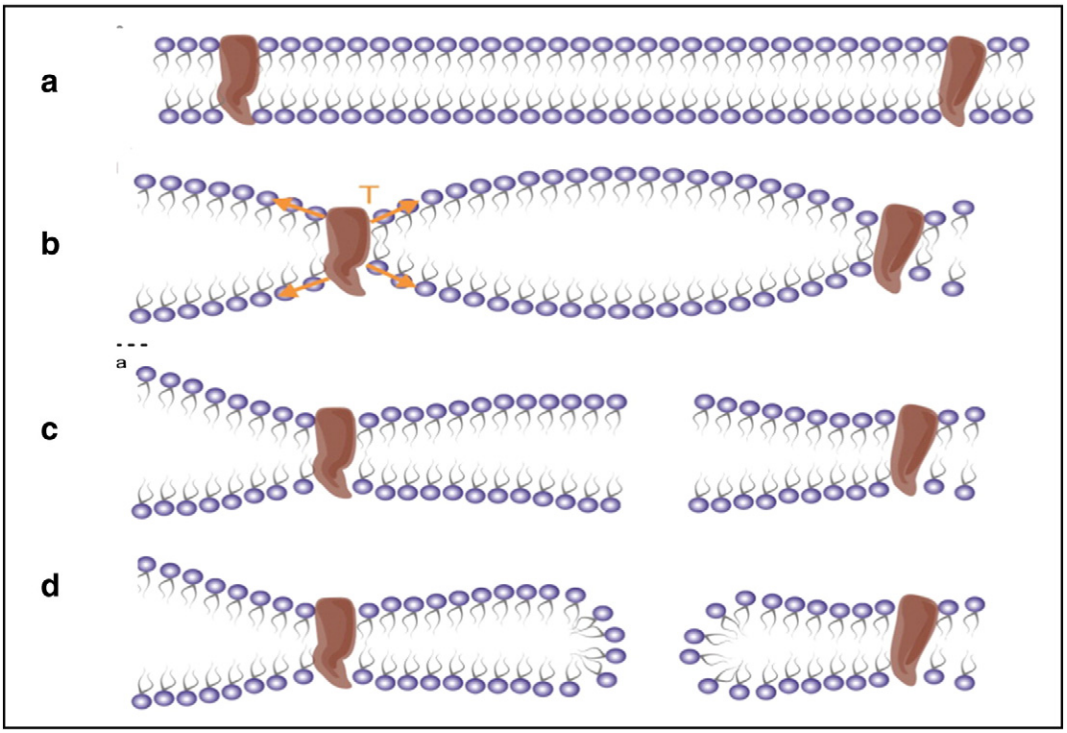

Fig. 9. A schematic representation of the BLS mechanism. A. Bilayer membrane; B. bilayer inflation during insonation; C. rupture of the bilayer membrane; D. channel formation. Adapted with permission from [24].

to determine the evolution of the gas channels under US irradiation. Their model's predictions qualitatively comply with experimental results.

Krasovitski et al. [24] in 2011 presented a cellular-level model, termed bilayer sonophore (BLS), describing the dynamic behavior of the two lipid bilayer membrane leaflets in an US pressure field (Fig. 9). They hypothesized that the intra-membrane hydrophobic space between the two lipid monolayer leaflets expands and contracts periodically when exposed to US. The two leaflets are pulled apart during the negative phase of the oscillating pressure when it overcomes the attractive forces between the leaflets and they are pushed back together during the positive phase of the pressure.

Their model predicts that this process can occur at both the diagnostic, non-thermal, non-cavitational and therapeutic, potentially cavitational spatial peak temporal average intensity levels. It shows that the bilayer membrane is capable of directly transforming acoustic energy into mechanical stresses and strains at the subcellular and cellular levels, which do not require prior existence of air voids in the tissue. The occurrence and behavior of BLSs in the membrane of the keratinocytes in the SC and their possible role in TDD sonophoresis remain to be studied.

4. Synergistic effects—recently, Polat et al. [92] in 2012 proposed a physical explanation of this phenomenon, suggesting that LFS enhances the penetration of CPEs into the skin. Using a mathematical model they showed that the transport flux of all CPEs is expected to increase the LTRs of LFS-treated skin. While in non-treated skin the CPE transport is solely caused by passive diffusion, the transport in LFS-treated skin is more complex. Here the impingements of collapsing bubble micro-jets within the LTRs are accounted for. The flux of a non-amphiphilic permeant into the skin depends on two contributions resulting from these micro-jets: (i) a convection-enhanced diffusional contribution due to the added mixing and streaming, and (ii) a contribution related to the quantity of bulk fluid injected into the skin with each micro-jet.

   In the case of a surface-active amphiphilic permeant, an additional contribution to the flux originates from the tendency of amphiphilic molecules to adsorb at the gas/water interface of the cavitation bubbles and the collapsing bubbles. When they collapse at the skin surface as cavitation micro-jets, these bubbles effectively deliver surfactants directly into the skin.

9. Safety issues

The FDA published in 1997 guidelines on ultrasound safety issues. The main parameters are the mechanical and thermal indices (MI and TI, respectively). These parameters and operating limitations are shown in Eqs. (3) and (4).

$$\mathrm{MI} = \frac{P_{r.3}(\mathrm{Z})}{\sqrt{\mathrm{f}}} \tag{3}$$

$$\mathrm{TI} = \frac{\mathrm{Wf}}{210}, \tag{4}$$

where f is the frequency in MHz, W is the bounded square output power (defined as the power emitted in the non-auto scanning mode from the contiguous one square centimeter of the active area of the transducer through which the highest ultrasonic power is transmitted) in mW/cm^2, and $P_{r.3}(Z)$ is the peak rarefactional pressure, derated by 0.3 dB/cm-MHz at each point along the beam axis (Z) [170]. The maximal value allowed for thermal index is 1.0, while the highest value for the mechanical index is 1.9 for most organs (except for ophthalmic procedures in which it is 0.23).

Another safety guideline, based on the intensity-time product of the form presented in Eq. (5), has been used to assess thermal damage threshold (mostly used for HIFU applications):

$$\mathrm{D} = \mathrm{I} \cdot \mathrm{t}^{\mathrm{m}} \tag{5}$$

where D is a tissue-dependent damage threshold, I is the average ISPTP spatial-peak temporal-average intensity, t is time, and m is a parameter

smaller than one [171]. Harris et al. [171] measured and found that m is between 0.3 and 0.8 and independent of the ultrasound frequency.

Collis et al. [163] provide another way to increase the sonoporation effect without increasing ultrasound intensity, thus avoiding potential safety issues. Their results suggest that appropriate tuning of the applied frequency may benefit therapeutic applications in terms of coverage and rates of sonoporation due to diversification of the induced shear stresses on the skin.

Another, yet a more minor, effect that may cause safety issues is the formation of free radicals as a result of cavitational bubble collapse. Sostaric et al. [172] found that using n-alkyl solutes (specifically glucopyranosides) in the medium completely inhibits cytolysis of insonated cells without decreasing inertial cavitation, thus eliminating the detrimental effect without affecting the beneficial effects. The findings of Saletes et al. [93] mentioned previously (40% reduction in intensity needed to induce inertial cavitation) may also be applied to reduce ultrasound intensity and thereby lower thermal effects without compromising the beneficial effects of ultrasound on enhanced transport (cavitation).

10. Synergistic effects of ultrasound

Ultrasound might enhance transport across skin by inducing skin alteration (thus decreasing its resistance to drug transport), as well as by inducing dynamic transport (forced convection) across the skin. Various other methods of transport enhancements, including chemical penetration enhancers [64,88,162,164,173], iontophoresis [174], and electroporation [175], might increase mass transport synergistically with ultrasound.

For example, Mitragotri et al. [68,162] assessed the synergistic effect of low-frequency ultrasound with chemical penetration enhancers (specifically surfactants), including SLS as a model permeate and mannitol. Insonation alone as well as SLS alone, both for 90 min, enhanced skin permeability approximately three fold for 1% SLS and eight fold for ultrasound. On the other hand, combining ultrasound with 1% SLS solution induced enhancement in skin permeability to mannitol nearly 200-fold. They suggest that the synergistic mechanism results from the increased penetration of SLS due to induced convection (resulting from cavitation) into the skin and into deeper layers. Polat et al. [88] investigated further the synergistic mechanism of LFS and SLS on mass transport across porcine skin. They found that the enhancement effect is not homogenous and consists of LTRs as in using LFS alone. They calculated from electrical conductivity experiments that pore radii created in LTRs were larger than 300 Å (for 20 kHz ultrasound). Interestingly, they found that new pores were also created in non-LTRs and that their calculated radii were ~18 Å (but still larger than pores found in untreated skin samples). They suggested that the enhanced transport mechanism within LTRs is caused by cavitation-induced micro-jets, whereas for non-LTRs the enhancement effect is probably due to SLS perturbations and increased penetration into the skin driven by ultrasound induced micro-streaming. Polat et al. suggest in another article [92] that since amphiphilic molecules tend to adsorb to cavitation bubble gas/water interface, the simultaneous application of SLS and LFS will result in an increased flux of amphiphilic versus non-amphiphilic molecules into the skin.

Lavon et al. [64] proposed that the synergistic effect observed for SLS and ultrasound when applied simultaneously can be also attributed to the modification of the pH profile in the SC when insonated: the altered pH profile increases SLS lipophilic solubility, penetration, and distribution.

Mutalik et al. examined the effect of ultrasound with CPEs for transdermal drug transport of 5% v/v citral in 50% v/v aqueous ethanol on the mass transport of tizanidine hydrochloride (TH) across mouse skin [176]. They found that the combined application yielded a synergistic effect (from a 0.025 mg cumulative quantity of TH in passive diffusion after 30 min to 2.459 mg using the combined effect). Ultrasound and CPEs were also used to enhance the mass transport of nanoparticles across mouse skin as was shown by Lee et al. [177] in the case of lanthanum nitrate ($LaNO_3$). The application that yielded the greatest enhancement in mass transport consisted of applying ultrasound (25 kHz) for 5 min at the intensity of 800 mW/cm^2 with 0.3 M of oleic acid (OA). The area density of $LaNO_3$, which penetrated into the viable epidermis, was about 18.4- and 1.84-fold higher in skin treated simultaneously with LFS and OA compared to that of skin treated separately with OA or LFS, respectively.

Not all CPEs show synergistic effects in combination with ultrasound. For example, El-Kamel et al. [178] found no enhancement of testosterone mass transport across rat skin when using low or high frequency ultrasound (20 kHz and 1–3 MHz, respectively) with 1% dodecylamine compared to using these applications separately. The authors offered no explanation as to why no synergistic or even additive effects exist.

Ultrasound also showed a synergistic effect with electroporation [69]: ultrasound decreased the threshold voltage required for electroporation and enhanced transdermal transport at a given electroporation voltage. The increase in transdermal transport induced by the combination of ultrasound and electroporation was greater than the additive enhancements induced by each enhancement method alone.

Combined application of ultrasound and iontophoresis has also applications of interest [174]. Their combination has a synergistic enhancement effect. As ultrasonic pretreatment decreases skin resistivity, a lower voltage is needed to deliver a permeate during iontophoresis compared to that in controls without ultrasound pretreatment. This ought to result in lower power requirements as well as less skin irritation. Hikima et al. explored the synergistic effects of sonophoresis and iontophoresis on skin penetration using vitamin B_{12} (molecular weight 1355.4 Da and non-ionized compound at physiological pH) as a model drug in the SC of hairless mice. They found that using ultrasound (3 MHz, 5.2 W/cm^2, 5.4% duty cycle) increased the penetration flux 12 times more than through intact skin; moreover, using IP (0.32 ± 0.3 mA/cm^2) increased the flux of VB_{12} 20 times compared to passive delivery. This enhancement refers to the increase in solubility and diffusivity of skin and convective water flow due to US and IP, respectively. A combination of US and IP has a synergistic effect of VB_{12} penetration. They proposed that the synergistic effect is caused by a different mechanism than the one caused by US or IP only for enhancing skin penetration, and that using a combination of US and IP is an effective means for delivering large molecules into the blood circulatory system [179]. In another paper they investigated the mechanism of skin penetration enhancement under sonophoresis or by IP on hairless mouse skin. They chose seven chemicals that differ in their molecular weight (122–1485 Da) as model compounds. The chemicals were dissolved in hydrophilic gel and loaded on the skin. The skin was separately treated by US or IP with the same parameters mentioned in the previous study, or by US + IP simultaneously. They found on the one hand, that the penetration profiles of ionized chemicals for US + IP were the same as for IP alone, but on the other hand, the penetration profiles of non-ionized chemicals synergistically increased for US + IP compared to US or IP separately. Moreover, chemicals with molecular weight less than 500 Da were influenced by IP while chemicals with molecular weight of more than 1000 Da showed synergistic effects with US + IP. They suggested that the synergistic effect of US + IP is mainly caused by an increase in the SC diffusivity and electro-osmotic water flow due to US and IP, respectively [180].

Ultrasound has also been used in combination with laser cell ablation technique. Terentyuk et al. [83] showed that the use of laser cell-ablation (erbium laser) can enable efficient delivery of gold nanoparticles (20–40 nm) across rat skin in vivo. These gold nanoparticles did not cross the skin without the use of enhancing techniques. They found that this enhancement effect was further increased when combined with 3 MHz ultrasound.

Recently, a combination of ultrasound and micro-needle array was developed [181]. Sonophoretic-enhanced micro-needle array (SEMA)

is used to deliver large molecular weight compounds through skin. This array consists of hollow micro-needles that pass the drug through the epidermis and into the dermis. Next, the fluid medium adjacent to the skin is exposed to ultrasound irradiation, inducing acoustic cavitation, which further facilitates the diffusion of large molecular compounds into the skin.

References

[1] M. Prausnitz, S.R. Mitragotri, R. Langer, Current status and future potential of transdermal drug delivery, Nat. Rev. Drug Discov. 3 (2004) 115–124.
[2] L. Chen, L. Han, G. Lian, Recent advances in predicting skin permeability of hydrophilic solutes, Adv. Drug Deliv. Rev. 65 (2013) 295–305.
[3] A.C. Williams, B.W. Barry, Penetration enhancers, Adv. Drug Deliv. Rev. 56 (2004) 603–618.
[4] S.E. Cross, M.S. Roberts, Physical enhancement of transdermal drug application: is delivery technology keeping up with pharmaceutical development? Curr. Drug Deliv. 12 (2004) 81–92.
[5] M.R. Prausnitz, Microneedles for transdermal drug delivery, Adv. Drug Deliv. Rev. 56 (2004) 581–587.
[6] W. Lee, T. Pan, P. Wang, R. Zhuo, C. Huang, J. Fang, Erbium:YAG laser enhances transdermal peptide delivery and skin vaccination, J. Controlled Release 128 (2008) 200–208.
[7] G. Levin, A. Gershonowitz, H. Sacks, M. Stern, A. Sherman, S. Rudaev, I. Zivin, M. Phillip, Transdermal delivery of human growth hormone through RF-microchannels, Pharm. Res. 22 (2005) 550–555.
[8] Y. Kam, H. Sacks, Keren Kaplan, M. Stern Mevorat, G. Levin, Radio frequency-microchannels for transdermal delivery: characterization of skin recovery and delivery window, Pharmacol. Pharm. 3 (2012) 20–28.
[9] Y.N. Kalia, A. Naik, J. Garrison, R.H. Guy, Iontophoretic drug delivery, Adv. Drug Deliv. Rev. 56 (2004) 619–658.
[10] Y. Wang, R. Thakur, Q. Fan, B. Michniak, Transdermal iontophoresis: combination strategies to improve transdermal iontophoretic drug delivery, Eur. J. Pharm. Biopharm. 60 (2005) 179–191.
[11] A. Denet, R. Vanbever, V. Préat, Skin electroporation for transdermal and topical delivery, Adv. Drug Deliv. Rev. 56 (2004) 659–674.
[12] H. Kalluri, A. Banga, Transdermal delivery of proteins, AAPS PharmSciTech 12 (2011) 431–441.
[13] A. Boucaud, Trends in the use of ultrasound-mediated transdermal drug delivery, Drug Discov. Today 9 (2004) 827–828.
[14] I. Lavon, J. Kost, Ultrasound and transdermal drug delivery, Drug Discov. Today 9 (2004) 670–676.
[15] M. Ogura, S. Paliwal, S. Mitragotri, Low-frequency sonophoresis: current status and future prospects, Adv. Drug Deliv. Rev. 60 (2008) 1218–1223.
[16] S. Mitragotri, Healing sound: the use of ultrasound in drug delivery and other therapeutic applications, Nat. Rev. Drug Discov. 4 (2005) 255–260.
[17] In: L. Lin (Ed.), Practical Clinical Ultrasonic Diagnosis, World Scientific Pub Co Inc., 1997
[18] G.t. Haar, C. Coussios, High intensity focused ultrasound: physical principles and devices, Int. J. Hyperth. 23 (2007) 89–104.
[19] Y.J. Wang, K.C. Leung, W. Cheung, H. Wang, L. Shi, D. Wang, L. Qin, A.T. Ahuja, Low-intensity pulsed ultrasound increases cellular uptake of superparamagnetic iron oxide nanomaterial: results from human osteosarcoma cell line U2OS, J. Magn. Reson. Imaging 31 (2010) 1508–1513.
[20] A. van Wamel, A. Bouakaz, B. Bernard, F. ten Cate, N. de Jong, Radionuclide tumour therapy with ultrasound contrast microbubbles, Ultrasonics 42 (2004) 903–906.
[21] K. Tachibana, T. Uchida, K. Tamura, H. Eguchi, N. Yamashita, K. Ogawa, Enhanced cytotoxic effect of Ara-C by low intensity ultrasound to HL-60 cells, Cancer Lett. 149 (2000) 189–194.
[22] J.C. Carmen, J.L. Nelson, B.L. Beckstead, C.M. Runyan, R.A. Robison, G.B. Schaalje, W.G. Pitt, Ultrasonic-enhanced gentamicin transport through colony biofilms of *Pseudomonas aeruginosa* and *Escherichia coli*, J. Infect. Chemother. 10 (2004) 193–199.
[23] E. Kimmel, Cavitation bioeffects, CRB 34 (2006) 105–161.
[24] B. Krasovitski, V. Frenkel, S. Shoham, E. Kimmel, Intramembrane cavitation as a unifying mechanism for ultrasound-induced bioeffects, Proc. Natl. Acad. Sci. 108 (2011) 3258–3263.
[25] L.H. Thompson, L.K. Doraiswamy, Sonochemistry: science and engineering, Ind. Eng. Chem. Res. 38 (1999) 1215–1249.
[26] K. Suslick, Ultrasound. Its Chemical, Physical, and Biological Effects, VCH, New York, 1989.
[27] S.A. Goss, R.L. Johnston, F. Dunn, Comprehensive compilation of empirical ultrasonic properties of mammalian tissues, J. Acoust. Soc. Am. 64 (1978) 423–457.
[28] W. Hendee R., E.R. Ritenour, Medical Imaging Physics, 4th edition Wiley-Liss, Canada, 2002.
[29] W.B. McNamara, Y.T. Didenko, K.S. Suslick, Sonoluminescence temperatures during multi-bubble cavitation, Nature 401 (1999) 772–775.
[30] W.B. McNamara, Y.T. Didenko, K.S. Suslick, Pressure during sonoluminescence, J. Phys. Chem. B 107 (2003) 7303–7306.
[31] D. Park, J. Yoon, J. Park, B. Jung, H. Park, J. Seo, Transdermal drug delivery aided by an ultrasound contrast agent: an in vitro experimental study, Open Biomed. Eng. J. 4 (2010).
[32] D. Park, H. Ryu, M. Namgung, K. Choi, Y. Kim, J. Seo, Sonophoresis with Ultrasound Contrast Agents in Transdermal Drug Delivery: In Vivo Experimental Study, Ultrasonics Symposium (IUS), 2010 IEEE, 2010, pp. 1575–1577.
[33] B.E. Polat, D. Hart, R. Langer, D. Blankschtein, Ultrasound-mediated transdermal drug delivery: mechanisms, scope, and emerging trends, J. Controlled Release 152 (2011) 330–348.
[34] M.S. Plesset, A. Prosperetti, Bubble dynamics and cavitation, Annu. Rev. Fluid Mech. 9 (1977) 145–185.
[35] B. Avvaru, A.B. Pandit, Oscillating bubble concentration and its size distribution using acoustic emission spectra, Ultrason. Sonochem. 16 (2009) 105–115.
[36] A. Brotchie, F. Grieser, M. Ashokkumar, Effect of power and frequency on bubble-size distributions in acoustic cavitation, Phys. Rev. Lett. 102 (2009) 084302.
[37] K.G. Baker, V.J. Robertson, F.A. Duck, A review of therapeutic ultrasound: biophysical effects, Phys. Ther. 81 (2001) 1351–1358.
[38] W.D. O'Brien Jr., Ultrasound — biophysics mechanisms, Prog. Biophys. Mol. Biol. 93 (2007) 212–255.
[39] D. Dalecki, Mechanical bioeffects of ultrasound, Annu. Rev. Biomed. Eng. 6 (2004) 229–248.
[40] L.B. Feril Jr., T. Kondo, Z. Cui, Y. Tabuchi, Q. Zhao, H. Ando, T. Misaki, H. Yoshikawa, S. Umemura, Apoptosis induced by the sonomechanical effects of low intensity pulsed ultrasound in a human leukemia cell line, Cancer Lett. 221 (2005) 145–152.
[41] N. Sekkat, Y.N. Kalia, R.H. Guy, Biophysical study of porcine ear skin in vitro and its comparison to human skin in vivo, J. Pharm. Sci. 91 (2002) 2376–2381.
[42] A. Boucaud, J. Montharu, L. Machet, B. Arbeille, M.C. Machet, F. Patat, L. Vaillant, Clinical, histologic, and electron microscopy study of skin exposed to low-frequency ultrasound, Anat. Rec. 264 (2001) 114–119.
[43] D. Steven, V. Shridhar, R.S. Anil, Effects of low frequency ultrasound on epidermal and dermal structures: a clinical and histological study, Cosmet. Dermatol. 19 (2006) 139–146.
[44] R.E. Gliklich, W. White, M.H. Slayton, P.G. Barthe, I.S. Makin, Clinical pilot study of intense ultrasound therapy to deep dermal facial skin and subcutaneous tissues, Arch. Facial Plast. Surg. 9 (2007) 88–95.
[45] D. Levy, J. Kost, Y. Meshulam, R. Langer, Effect of ultrasound on transdermal drug delivery to rats and guinea pigs, J. Clin. Invest. 83 (1989) 2074–2078.
[46] K. Tachibana, Transdermal delivery of insulin to alloxan-diabetic rabbits by ultrasound exposure, Pharm. Res. 9 (1992) 952–954.
[47] S. Mitragotri, D. Blankschtein, R. Langer, Ultrasound-mediated transdermal protein delivery, Science 269 (1995) 850–853.
[48] S. Mitragotri, D. Blankschtein, R. Langer, Transdermal drug delivery using low-frequency sonophoresis, Pharm. Res. 13 (1996) 411–420.
[49] N. Yamashita, K. Tachibana, K. Ogawa, N. Tsujita, A. Tomita, Scanning electron microscopic evaluation of the skin surface after ultrasound exposure, Anat. Rec. 247 (1997) 455–461.
[50] A. Boucaud, L. Machet, B. Arbeille, M.C. Machet, M. Sournac, A. Mavon, F. Patat, L. Vaillant, In vitro study of low-frequency ultrasound-enhanced transdermal transport of fentanyl and caffeine across human and hairless rat skin, Int. J. Pharm. 228 (2001) 69–77.
[51] J. Voigt, M. Wendelken, V. Driver, O.M. Alvarez, Low-frequency ultrasound (20–40 kHz) as an adjunctive therapy for chronic wound healing: a systematic review of the literature and meta-analysis of eight randomized controlled trials, Int. J. Low. Extrem. Wounds 10 (2011) 190–199.
[52] L.J. Bond, W.W. Cimino, Physics of ultrasonic surgery using tissue fragmentation: part II, Ultrasound Med. Biol. 22 (1996) 101–117.
[53] R. Gurfinkel, I. Lavon, E. Cagnano, K. Volgin, L. Shaltiel, N. Grossman, J. Kost, A.J. Singer, L. Rosenberg, Combined ultrasonic and enzymatic debridement of necrotic eschars in an animal model, J. Burn Care Res. 30 (2009).
[54] J. Moreno-Moraga, T. Valero-Altés, A.M. Riquelme, M.I. Isarria-Marcosy, J.R. de la Torre, Body contouring by non-invasive transdermal focused ultrasound, Lasers Surg. Med. 39 (2007) 315–323.
[55] B. Ascher, Safety and efficacy of UltraShape Contour I treatments to improve the appearance of body contours: multiple treatments in shorter intervals, Aesthet. Surg. J. 30 (2010) 217–224.
[56] S. Shek, C. Yu, C.K. Yeung, T. Kono, H.H. Chan, The use of focused ultrasound for non-invasive body contouring in Asians, Lasers Surg. Med. 41 (2009) 751–759.
[57] E.A. White, A. Horne, J. Runciman, M.E. Orazem, W.C. Navidi, C.S. Roper, A.L. Bunge, On the correlation between single-frequency impedance measurements and human skin permeability to water, Toxicol. in Vitro 25 (2011) 2095–2104.
[58] W.W. Makin, Selective creation of thermal injury zones in the superficial musculoaponeurotic system using intense ultrasound therapy: a new target for noninvasive facial rejuvenation, Arch. Facial Plast. Surg. 9 (2007) 22–29.
[59] K. Fellinger, J. Schmidt, Klinik and therapies des chromischen gelenkreumatismus, Anonymous, Vienna, 1954.
[60] The Sontra Medical, SonoPrep® Ultrasonic Skin Permeation System and Procedure Tray, K023713, 2004.
[61] A. Boucaud, M.A. Garrigue, L. Machet, L. Vaillant, F. Patat, Effect of sonication parameters on transdermal delivery of insulin to hairless rats, J. Controlled Release 81 (2002) 113–119.
[62] T. Terahara, S. Mitragotri, R. Langer, Porous resins as a cavitation enhancer for low-frequency sonophoresis, J. Pharm. Sci. 91 (2002) 753–759.
[63] T. Terahara, S. Mitragotri, J. Kost, R. Langer, Dependence of low-frequency sonophoresis on ultrasound parameters; distance of the horn and intensity, Int. J. Pharm. 235 (2002) 35–42.
[64] I. Lavon, N. Grossman, J. Kost, The nature of ultrasound—SLS synergism during enhanced transdermal transport, J. Controlled Release 107 (2005) 484–494.
[65] N.P. Katz, D.E. Shapiro, T.E. Herrmann, J. Kost, L.M. Custer, Rapid onset of cutaneous anesthesia with EMLA cream after pretreatment with a new ultrasound-emitting device, Anesth. Analg. 98 (2004) 371–376.
[66] J. Kost, S. Mitragotri, R.A. Gabbay, M. Pishko, R. Langer, Transdermal monitoring of glucose and other analytes using ultrasound, Nat. Med. 6 (2000) 347–350.

[67] A. Tezel, S. Paliwal, Z. Shen, S. Mitragotri, Low-frequency ultrasound as a transcutaneous immunization adjuvant, Vaccine 23 (2005) 3800–3807.
[68] S. Mitragotri, D. Ray, J. Farrell, H. Tang, B. Yu, J. Kost, D. Blankschtein, R. Langer, Synergistic effect of low-frequency ultrasound and sodium lauryl sulfate on transdermal transport, J. Pharm. Sci. 89 (2000) 892–900.
[69] J. Kost, U. Pliquett, S. Mitragotri, A. Yamamoto, R. Langer, J. Weaver, Synergistic effect of electric field and ultrasound on transdermal transport, Pharm. Res. 13 (1996) 633–638.
[70] A. Tezel, S. Dokka, S. Kelly, G.E. Hardee, S. Mitragotri, Topical delivery of anti-sense oligonucleotides using low-frequency sonophoresis, Pharm. Res. 21 (2004) 2219–2225.
[71] A. Tezel, S. Mitragotri, Interactions of inertial cavitation bubbles with stratum corneum lipid bilayers during low-frequency sonophoresis, Biophys. J. 85 (2003) 3502–3512.
[72] D. Bommannan, H. Okuyama, P. Stauffer, R. Guy, Sonophoresis. I. The use of high-frequency ultrasound to enhance transdermal drug delivery, Pharm. Res. 9 (1992) 559–564.
[73] D. Bommannan, G.K. Menon, H. Okuyama, P.M. Elias, R.H. Guy, Sonophoresis. II. Examination of the mechanism(s) of ultrasound-enhanced transdermal drug delivery, Pharm. Res. 9 (1992) 1043–1047.
[74] G. Menon, D. Bommannan, P. Elias, High-frequency sonophoresis: permeation pathways and structural basis for enhanced permeability, Skin Pharmacol. 7 (1994) 130–139.
[75] J. Fang, C. Fang, K.C. Sung, H. Chen, Effect of low frequency ultrasound on the in vitro percutaneous absorption of clobetasol 17-propionate, Int. J. Pharm. 191 (1999) 33–42.
[76] M. Mutoh, H. Ueda, Y. Nakamura, K. Hirayama, M. Atobe, D. Kobayashi, Y. Morimoto, Characterization of transdermal solute transport induced by low-frequency ultrasound in the hairless rat skin, J. Controlled Release 92 (2003) 137–146.
[77] S. Mitragotri, J. Kost, Transdermal delivery of heparin and low-molecular weight heparin using low-frequency ultrasound, Pharm. Res. 18 (2001) 1151–1156.
[78] S. Katikaneni, G. Li, A. Badkar, A.K. Banga, Transdermal delivery of a 13 kDa protein—an in vivo comparison of physical enhancement methods, J. Drug Target. 18 (2010) 141–147.
[79] H. Liu, S. Li, W. Pan, Y. Wang, F. Han, H. Yao, Investigation into the potential of low-frequency ultrasound facilitated topical delivery of Cyclosporin A, Int. J. Pharm. 326 (2006) 32–38.
[80] A. Maruani, E. Vierron, L. Machet, B. Giraudeau, A. Boucaud, Efficiency of low-frequency ultrasound sonophoresis in skin penetration of histamine: a randomized study in humans, Int. J. Pharm. 385 (2010) 37–41.
[81] R.F.V. Lopez, J.E. Seto, D. Blankschtein, R. Langer, Enhancing the transdermal delivery of rigid nanoparticles using the simultaneous application of ultrasound and sodium lauryl sulfate, Biomaterials 32 (2011) 933–941.
[82] J.E. Seto, B.E. Polat, R.F.V. Lopez, D. Blankschtein, R. Langer, Effects of ultrasound and sodium lauryl sulfate on the transdermal delivery of hydrophilic permeants: comparative in vitro studies with full-thickness and split-thickness pig and human skin, J. Controlled Release 145 (2010) 26–32.
[83] G.S. Terentyuk, Elina A. Genina, A.N. Bashkatov, M.V. Ryzhova, N.A. Tsyganova, D.S. Chumakov, B.N. Khlebtsov, A.A. Sazonov, L.E. Dolotov, Valerii V. Tuchin, Nikolai G. Khlebtsov, O.A. Inozemtseva, Use of fractional laser microablation and ultrasound to facilitate the delivery of gold nanoparticles into skin in vivo, Quantum Electron. 42 (2012) 471.
[84] S. Mutalik, U.Y. Nayak, R. Kalra, A. Kumar, R.V. Kulkarni, H.S. Parekh, Sonophoresis-mediated permeation and retention of peptide dendrimers across human epidermis, Skin Res. Technol. 18 (2012) 101–107.
[85] B. Cagnie, E. Vinck, S. Rimbaut, G. Vanderstraeten, Phonophoresis versus topical application of ketoprofen: comparison between tissue and plasma levels, Phys. Ther. 83 (2003) 707–712.
[86] K. Tachibana, S. Tachibana, Transdermal delivery of insulin by ultrasonic vibration, J. Pharm. Pharmacol. 43 (1991) 270–271.
[87] H. Ueda, M. Mutoh, T. Seki, D. Kobayashi, Y. Morimoto, Acoustic cavitation as an enhancing mechanism of low-frequency sonophoresis for transdermal drug delivery, Biol. Pharm. Bull. 32 (2009) 916–920.
[88] B.E. Polat, P.L. Figueroa, D. Blankschtein, R. Langer, Transport pathways and enhancement mechanisms within localized and non-localized transport regions in skin treated with low-frequency sonophoresis and sodium lauryl sulfate, J. Pharm. Sci. 100 (2011) 512–529.
[89] C.M. Schoellhammer, B.E. Polat, J. Mendenhall, R. Maa, B. Jones, D.P. Hart, R. Langer, D. Blankschtein, Rapid skin permeabilization by the simultaneous application of dual-frequency, high-intensity ultrasound, J. Controlled Release 163 (2012) 154–160.
[90] H. Liu, C. Hsieh, Single-transducer dual-frequency ultrasound generation to enhance acoustic cavitation, Ultrason. Sonochem. 16 (2009) 431–438.
[91] A. Brotchie, R. Mettin, F. Grieser, M. Ashokkumar, Cavitation activation by dual-frequency ultrasound and shock waves, Phys. Chem. Chem. Phys. 11 (2009) 10029–10034.
[92] B.E. Polat, W.M. Deen, R. Langer, D. Blankschtein, A physical mechanism to explain the delivery of chemical penetration enhancers into skin during transdermal sonophoresis—insight into the observed synergism, J. Controlled Release 158 (2012) 250–260.
[93] I. Saletes, B. Gilles, J. Bera, E.S. Ebbini, Lowering cavitation threshold using bifrequency excitation: nonlinear aspect and influence of the difference frequency, AIP 1113 (2009) 53–57.
[94] T. Hikima, Y. Hirai, K. Tojo, Effect of ultrasound application on skin metabolism of prednisolone 21-acetate, Pharm. Res. 15 (1998) 1680–1683.
[95] R. Rekha, N. Sanju, A.B. Nair, Influence of ultrasound mediated transdermal delivery of losartan potassium, Drug Deliv. Lett. 2 (2012) 46–53.
[96] O. Sarheed, B.K.A. Rasool, Development of an optimised application protocol for sonophoretic transdermal delivery of a model hydrophilic drug, Open Biomed. Eng. J. 15 (2011) 14–24.
[97] N.B. Smith, S. Lee, E. Maione, R.B. Roy, S. McElligott, K.K. Shung, Ultrasound-mediated transdermal transport of insulin in vitro through human skin using novel transducer designs, Ultrasound Med. Biol. 29 (2003) 311–317.
[98] N.B. Smith, S. Lee, K.K. Shung, Ultrasound-mediated transdermal in vivo transport of insulin with low-profile cymbal arrays, Ultrasound Med. Biol. 29 (2003) 1205–1210.
[99] S. Lee, R.E. Newnham, N.B. Smith, Short ultrasound exposure times for noninvasive insulin delivery in rats using the lightweight cymbal array, IEEE Trans. Ultrason. Ferroelectr. Freq. Control. 51 (2004) 176–180.
[100] S. Lee, B. Snyder, R.J. Meyer, V. Nayak, D. Markley, R.E. Newnham, N.B. Smith, Non-invasive Ultrasonic Transdermal Insulin Delivery in Rabbits Using the Light Weight Cymbal Array, Ultrasonics, 2003 IEEE Symposium on 1, Vol.1, 2003, pp. 736–739.
[101] E.J. Park, J. Werner, N. Smith, Ultrasound mediated transdermal insulin delivery in pigs using a lightweight transducer, Pharm. Res. 24 (2007) 1396–1401.
[102] E.J. Park, J. Dodds, N.B. Smith, Dose comparison of ultrasonic transdermal insulin delivery to subcutaneous insulin injection, Int. J. Nanomedicine 3 (2008) 335–341.
[103] A. Elbakry, A. Zaky, R. Liebl, R. Rachel, A. Goepferich, M. Breunig, Layer-by-layer assembled gold nanoparticles for siRNA delivery, Nano Lett. 9 (2009) 2059–2064.
[104] J. Luis, E.J. Park, Richard J. Meyer, N.B. Smith, Rectangular cymbal arrays for improved ultrasonic transdermal insulin delivery, J. Acoust. Soc. Am. 122 (2007) 2022–2030.
[105] S. Mitragotri S., J. Kost, S. Kellogg C., N. Warner F., A. Elstrom Tuan, Method and apparatus for enhancement of transdermal transport, US 10/792,862 (2012) 1–41.
[106] S. Mitragotri, J. Kost, Low-frequency sonophoresis: a review, Adv. Drug Deliv. Rev. 56 (2004) 589–601.
[107] M. Meshali, H. Abdel-Aleem, F. Sakr, S. Nazzal, Y. El-Malah, Effect of gel composition and phonophoresis on the transdermal delivery of ibuprofen: in vitro and in vivo evaluation, Pharm. Dev. Technol. 16 (2011) 93–101.
[108] B.M. Becker, S. Helfrich, E. Baker, K. Lovgren, P.A. Minugh, J.T. Machan, Ultrasound with topical anesthetic rapidly decreases pain of intravenous cannulation, Acad. Emerg. Med. 12 (2005) 289–295.
[109] S. Skarbek-Borowska, B.M. Becker, K. Lovgren, A. Bates, P.A. Minugh, Brief focal ultrasound with topical anesthetic decreases the pain of intravenous placement in children, Pediatr. Emerg. Care 22 (2006).
[110] J. Gupta, M.R. Prausnitz, Recovery of skin barrier properties after sonication in human subjects, Ultrasound Med. Biol. 35 (2009) 1405–1408.
[111] G. Krishnan, J.E. Grice, M.S. Roberts, H.A.E. Benson, T.W. Prow, Enhanced sonophoretic delivery of 5-aminolevulinic acid: preliminary human ex vivo permeation data, Skin Res. Technol. 19 (2013) e283–e289.
[112] S. Mitragotri, Devices for overcoming biological barriers: the use of physical forces to disrupt the barriers, Adv. Drug Deliv. Rev. 65 (2013) 100–103.
[113] T. Singh, M. Garland, C. Cassidy, K. Migalska, Y. Demir, S. Abdelghany, E. Ryan, A. Woolfson, R. Donnelly, Microporation techniques for enhanced delivery of therapeutic agents, Recent Pat. Drug Deliv. Formul. 4 (2010) 1–17.
[114] R. Seip, Therapeutic ultrasound research and development from an industrial and commercial perspective, AIP Conf. Proc. 1113 (2009) 323–326.
[115] G. Kasting, L. Bowman, DC electrical properties of frozen, excised human skin, Pharm. Res. 7 (1990) 134–143.
[116] A. Tezel, A. Sens, S. Mitragotri, Description of transdermal transport of hydrophilic solutes during low-frequency sonophoresis based on a modified porous pathway model, J. Pharm. Sci. 92 (2003) 381–393.
[117] P. Karande, A. Jain, S. Mitragotri, Discovery of transdermal penetration enhancers by high-throughput screening, Nat. Biotechnol. 22 (2004) 192–197.
[118] H. Chuang, E. Taylor, T.W. Davison, Clinical evaluation of a continuous minimally invasive glucose flux sensor placed over ultrasonically permeated skin, Diabetes Technol. Ther. 6 (2004) 21–30.
[119] R. Alvarez-Román, G. Merino, Y.N. Kalia, A. Naik, R.H. Guy, Skin permeability enhancement by low frequency sonophoresis: lipid extraction and transport pathways, J. Pharm. Sci. 92 (2003) 1138–1146.
[120] C.M. Gockel, S. Bao, K.W. Beagley, Transcutaneous immunization induces mucosal and systemic immunity: a potent method for targeting immunity to the female reproductive tract, Mol. Immunol. 37 (2000) 537–544.
[121] S. Babiuk, M. Baca-Estrada, L.A. Babiuk, C. Ewen, M. Foldvari, Cutaneous vaccination: the skin as an immunologically active tissue and the challenge of antigen delivery, J. Controlled Release 66 (2000) 199–214.
[122] N. Romani, S. Holzmann, C.H. Tripp, F. Koch, P. Stoitzner, Langerhans cells—dendritic cells of the epidermis, APMIS 111 (2003) 725–740.
[123] P. Stoitzner, S. Holzmann, A.D. McLellan, L. Ivarsson, H. Stossel, M. Kapp, U. Kammerer, P. Douillard, E. Kampgen, F. Koch, S. Saeland, N. Romani, Visualization and characterization of migratory Langerhans cells in murine skin and lymph nodes by antibodies against Langerin/CD207, J. Investig. Dermatol. 120 (2003) 266–274.
[124] G.M. Glenn, T. Scharton-Kersten, R. Vassell, C.P. Mallett, T.L. Hale, C.R. Alving, Cutting edge: transcutaneous immunization with cholera toxin protects mice against lethal mucosal toxin challenge, J. Immunol. 161 (1998) 3211–3214.
[125] G.M. Glenn, R.T. Kenney, in: S. Plotkin (Ed.), Mass Vaccination: Solutions in the Skin, Springer, Berlin Heidelberg, 2006, pp. 247–268.
[126] A. Dahlan, H.O. Alpar, P. Stickings, D. Sesardic, S. Murdan, Transcutaneous immunisation assisted by low-frequency ultrasound, Int. J. Pharm. 368 (2009) 123–128.
[127] A. Dahlan, H.O. Alpar, S. Murdan, An investigation into the combination of low frequency ultrasound and liposomes on skin permeability, Int. J. Pharm. 379 (2009) 139–142.
[128] T. Cao, X. Wang, D. Roop, Regulated cutaneous gene delivery: the skin as a bioreactor, Hum. Gene Ther. 11 (2000) 2297–2300.

[129] C. Featherstone, J. Uitto, Ex vivo gene therapy cures a blistering skin disease, Trends Mol. Med. 13 (2007) 219–222.
[130] D.M. Frerichs, L.R. Ellingsworth, S.A. Frech, D.C. Flyer, C.P. Villar, J. Yu, G.M. Glenn, Controlled, single-step, stratum corneum disruption as a pretreatment for immunization via a patch, Vaccine 26 (2008) 2782–2787.
[131] J. Uitto, L. Pulkkinen, The genodermatoses: candidate diseases for gene therapy, Hum. Gene Ther. 11 (2000) 2267–2275.
[132] S. Hammond, M. Guebre-Xabier, J. Yu, G. Glenn, Transcutaneous immunization: an emerging route of immunization and potent immunostimulation strategy, Crit. Rev. Ther. Drug Carrier Syst. 18 (2001) 503–526.
[133] S. Özbaş-Turan, J. Akbuğa, Plasmid DNA-loaded chitosan/TPP nanoparticles for topical gene delivery, Drug Deliv. 18 (2011) 215–222.
[134] M.A. Tran, R. Gowda, A. Sharma, E. Park, J. Adair, M. Kester, N.B. Smith, G.P. Robertson, Targeting V600EB-Raf and Akt3 using nanoliposomal-small interfering RNA inhibits cutaneous melanocytic lesion development, Cancer Res. 68 (2008) 7638–7649.
[135] D. Zheng, D.A. Giljohann, D.L. Chen, M.D. Massich, X. Wang, H. Iordanov, C.A. Mirkin, A.S. Paller, Topical delivery of siRNA-based spherical nucleic acid nanoparticle conjugates for gene regulation, Proc. Natl. Acad. Sci. 109 (no. 30) (2012) 11975–11980.
[136] P. Ritprajak, M. Hashiguchi, M. Azuma, Topical application of cream-emulsified CD86 siRNA ameliorates allergic skin disease by targeting cutaneous dendritic cells, Mol. Ther. 16 (2008) 1323–1330.
[137] S. Nikol, I. Baumgartner, E. Van Belle, C. Diehm, A. Visona, M.C. Capogrossi, N. Ferreira-Maldent, A. Gallino, M. Graham Wyatt, L. Dinesh Wijesinghe, M. Fusari, D. Stephan, J. Emmerich, G. Pompilio, F. Vermassen, E. Pham, V. Grek, M. Coleman, F. Meyer, Therapeutic angiogenesis with intramuscular NV1FGF improves amputation-free survival in patients with critical limb ischemia, Mol. Ther. 16 (2008) 972–978.
[138] R.J. Powell, M. Simons, F.O. Mendelsohn, G. Daniel, T.D. Henry, M. Koga, R. Morishita, B.H. Annex, Results of a double-blind, placebo-controlled study to assess the safety of intramuscular injection of hepatocyte growth factor plasmid to improve limb perfusion in patients with critical limb ischemia, Circulation 118 (2008) 58–65.
[139] Q. Jiang, J. Uitto, Animal models of epidermolysis bullosa—targets for gene therapy, J. Investig. Dermatol. 124 (2005) xi–xiii.
[140] J. Uitto, Epidermolysis bullosa: prospects for cell-based therapies, J. Investig. Dermatol. 128 (2008) 2140–2142.
[141] M.A. Tran, R. Gowda, E. Park, J. Adair, N. Smith, Mark Kester, Gavin P. Robertson, Noninvasive drug delivery using ultrasound: targeting melanoma using siRNA against mutant (V600E) B-Raf, AIP Conf. Proc. 1113 (2009) 423–429.
[142] B. Geusens, T. Strobbe, S. Bracke, P. Dynoodt, N. Sanders, M.V. Gele, J. Lambert, Lipid-mediated gene delivery to the skin, Eur. J. Pharm. Sci. 43 (2011) 199–211.
[143] Y. Liu, J. Yan, M.R. Prausnitz, Can ultrasound enable efficient intracellular uptake of molecules? A retrospective literature review and analysis, Ultrasound Med. Biol. 38 (2012) 876–888.
[144] A. Sieg, R. Guy, M. Delgado-Charro, Noninvasive and minimally invasive methods for transdermal glucose monitoring, Diabetes Technol. Ther. 7 (2005) 174–197.
[145] H. Chuang, M. Trieu, J. Hurley, E.J. Taylor, M.R. England, S.A.J. Nasraway, Pilot studies of transdermal continuous glucose measurement in outpatient diabetic patients and in patients during and after cardiac surgery, J. Diabetes Sci. Technol. 2 (2008) 595–602.
[146] H. Yu, J. Liu, T. Shi, D. Li, Z. Du, K. Xu, Using Skin Impedance to Improve Prediction Accuracy of Continuous Glucose Monitoring System, 2008. 68630S–S.
[147] E. Park, J. Werner, D. Jaiswal, N.B. Smith, K. Hynynen, J. Souquet, Closed-loop controlled noninvasive ultrasonic glucose sensing and insulin delivery, AIP Conf. Proc. 1215 (2010) 157–160.
[148] J. Simonin, On the mechanisms of in vitro and in vivo phonophoresis, J. Controlled Release 33 (1995) 125–141.
[149] H. Tang, S. Mitragotri, D. Blankschtein, R. Langer, Theoretical description of transdermal transport of hydrophilic permeants: application to low-frequency sonophoresis, J. Pharm. Sci. 90 (2001) 545–568.
[150] I. Lavon, N. Grossman, J. Kost, E. Kimmel, G. Enden, Bubble growth within the skin by rectified diffusion might play a significant role in sonophoresis, J. Controlled Release 117 (2007) 246–255.
[151] S. Mitragotri, D. Edwards, D. Blankschtein, R. Langer, A mechanistic study of ultrasonically-enhanced transdermal drug delivery, J. Pharm. Sci. 84 (1995) 697–706.
[152] P. Karande, A. Jain, K. Ergun, V. Kispersky, S. Mitragotri, Design principles of chemical penetration enhancers for transdermal drug delivery, Proc. Natl. Acad. Sci. U. S. A. 102 (2005) 4688–4693.
[153] L. Wolloch, J. Kost, The importance of microjet vs shock wave formation in sonophoresis, J. Controlled Release 148 (2010) 204–211.
[154] A. Tezel, A. Sens, J. Tuchscherer, S. Mitragotri, Frequency dependence of sonophoresis, Pharm. Res. 18 (2001) 1694–1700.
[155] J. Kushner, D. Blankschtein, R. Langer, Experimental demonstration of the existence of highly permeable localized transport regions in low-frequency sonophoresis, J. Pharm. Sci. 93 (2004) 2733–2745.
[156] J. Kushner, D. Blankschtein, R. Langer, Evaluation of the porosity, the tortuosity, and the hindrance factor for the transdermal delivery of hydrophilic permeants in the context of the aqueous pore pathway hypothesis using dual-radiolabeled permeability experiments, J. Pharm. Sci. 96 (2007) 3263–3282.
[157] J. Kushner, D. Blankschtein, R. Langer, Evaluation of hydrophilic permeant transport parameters in the localized and non-localized transport regions of skin treated simultaneously with low-frequency ultrasound and sodium lauryl sulfate, J. Pharm. Sci. 97 (2008) 906–918.
[158] J. Kushner, D. Blankschtein, R. Langer, Heterogeneity in skin treated with low-frequency ultrasound, J. Pharm. Sci. 97 (2008) 4119–4128.
[159] J. Kushner IV, D. Kim, P.T.C. So, D. Blankschtein, R.S. Langer, Dual-channel two-photon microscopy study of transdermal transport in skin treated with low-frequency ultrasound and a chemical enhancer, J. Investig. Dermatol. 127 (2007) 2832–2846.
[160] S. Paliwal, K.M. Gopinathan, S. Mitragotri, Low-frequency sonophoresis: ultrastructural basis for stratum corneum permeability assessed using quantum dots, J. Investig. Dermatol. 126 (2006) 1095–1101.
[161] G. Merino, Y.N. Kalia, M.B. Delgado-Charro, R.O. Potts, R.H. Guy, Frequency and thermal effects on the enhancement of transdermal transport by sonophoresis, J. Controlled Release 88 (2003) 85–94.
[162] A. Tezel, A. Sens, J. Tuchscherer, S. Mitragotri, Synergistic effect of low-frequency ultrasound and surfactants on skin permeability, J. Pharm. Sci. 91 (2002) 91–100.
[163] J. Collis, R. Manasseh, P. Liovic, P. Tho, A. Ooi, K. Petkovic-Duran, Y. Zhu, Cavitation microstreaming and stress fields created by microbubbles, Ultrasonics 50 (2010) 273–279.
[164] A. Tezel, A. Sens, S. Mitragotri, Investigations of the role of cavitation in low-frequency sonophoresis using acoustic spectroscopy, J. Pharm. Sci. 91 (2002) 444–453.
[165] I.P. Dick, R.C. Scott, Pig ear skin as an in-vitro model for human skin permeability, J. Pharm. Pharmacol. 44 (1992) 640–645.
[166] L.M. Cancel, J.M. Tarbell, A. Ben-Jebria, Fluorescein permeability and electrical resistance of human skin during low frequency ultrasound application, J. Pharm. Pharmacol. 59 (2004) 1109–1118.
[167] Y. Morimoto, M. Mutoh, H. Ueda, L. Fang, K. Hirayama, M. Atobe, D. Kobayashi, Elucidation of the transport pathway in hairless rat skin enhanced by low-frequency sonophoresis based on the solute–water transport relationship and confocal microscopy, J. Controlled Release 103 (2005) 587–597.
[168] S.S.S. Lanke, C.S. Kolli, J.G. Strom, A.K. Banga, Enhanced transdermal delivery of low molecular weight heparin by barrier perturbation, Int. J. Pharm. 365 (2009) 26–33.
[169] S. Mitragotri, Y.G. Anissimov, A.L. Bunge, H.F. Frasch, R.H. Guy, J. Hadgraft, G.B. Kasting, M.E. Lane, M.S. Roberts, Mathematical models of skin permeability: an overview, Int. J. Pharm. 418 (2011) 115–129.
[170] Guidance for Industry and FDA Staff, Information for Manufacturers Seeking Marketing Clearance of Diagnostic Ultrasound Systems and Transducers, 1997.
[171] G.R. Harris, B.A. Herman, M.R. Myers, An analytical comparison of the thermal dose equation and the intensity-time product, Itm, for predicting tissue damage thresholds, AIP Conf. Proc. 1215 (2010) 136–241.
[172] J.Z. Sostaric, N. Miyoshi, P. Riesz, W.G. De Graff, J.B. Mitchell, Complete inhibition of ultrasound induced cytolysis in the presence of inertial cavitation, AIP Conf. Proc. 826 (2006) 39–45.
[173] M.E. Johnson, S. Mitragotri, A. Patel, D. Blankschtein, R. Langer, Synergistic effects of chemical enhancers and therapeutic ultrasound on transdermal drug delivery, J. Pharm. Sci. 85 (1996) 670–679.
[174] L. Le, J. Kost, S. Mitragotri, Combined effect of low-frequency ultrasound and iontophoresis: applications for transdermal heparin delivery, Pharm. Res. 17 (2000) 1151–1154.
[175] I. Kim, A. Dunkhorst, J. Gilbert, U.H.F. Bunz, Sensing of lead ions by a carboxylate-substituted PPE: multivalency effects, Macromolecules 38 (2005) 4560–4562.
[176] S. Mutalik, H.S. Parekh, N.M. Davies, U. Nayanabhirama, A combined approach of chemical enhancers and sonophoresis for the transdermal delivery of tizanidine hydrochloride, Drug Deliv. 16 (2009) 82–91.
[177] S.E. Lee, K.J. Choi, G.K. Menon, H.J. Kim, E.H. Choi, S.K. Ahn, S.H. Lee, Penetration pathways induced by low-frequency sonophoresis with physical and chemical enhancers: iron oxide nanoparticles versus lanthanum nitrates, J. Investig. Dermatol. 130 (2010) 1063–1072.
[178] A. El-Kamel, I. Al-Fagih, I. Alsarra, Effect of sonophoresis and chemical enhancers on testosterone transdermal delivery from solid lipid microparticles: an in vitro study, Curr. Drug Deliv. 5 (2008) 20–26.
[179] K. Shirouzu, T. Nishiyama, T. Hikima, K. Tojo, Synergistic effect of sonophoresis and iontophoresis in transdermal drug delivery, J. Chem. Eng. Jpn. 41 (2008) 300–305.
[180] T. Hikima, S. Ohsumi, K. Shirouzu, K. Tojo, Mechanisms of synergistic skin penetration by sonophoresis and iontophoresis, Biol. Pharm. Bull. 32 (2009) 905–909.
[181] B. Chen, J. Wei, C. Iliescu, Sonophoretic enhanced microneedles array (SEMA)—improving the efficiency of transdermal drug delivery, Sensors Actuators B Chem. 145 (2010) 54–60.